

## A History of Coal Liquefaction in United Kingdom, 1967-1992

Geoff M. Kimber  
Coal Science & Technology Consultant  
(formerly Technical Manager, British Coal Corporation  
Liquefaction Project)

20 King William Drive  
Cheltenham  
Gloucs. GL53 7RP  
United Kingdom

**Keywords:** Coal, Liquefaction, U.K. History 1967-1992.

### **ABSTRACT**

This paper gives an overview of the coal liquefaction studies carried out by the British Coal Utilisation Research Association, (BCURA), the National Coal Board (NCB), and the British Coal Corporation (BCC), between 1967 and 1992 at their research establishments in Leatherhead, Stoke Orchard and Point of Ayr. It is based upon a recently published ~100 page report<sup>(1)</sup> which condensed into a single reference document the contents of several hundred internal reports not generally available outside of BCC.

### **INTRODUCTION**

Coal liquefaction is not new. Although Berthelot observed as early as 1869 that coal could be converted to an oil-like product by chemical reduction, practical processes using hydrogenation really date from 1913, when Bergius showed that brown coal could be converted to a heavy crude oil.

The main early developments took place during the 1920s and 1930s in Germany, while in the U.K. Imperial Chemical Industries built a plant at Billingham to produce 100,000t/year of liquid fuels from bituminous coal. This operated until 1939, after which it was used instead to convert creosote oil to aviation fuel. At this time, Germany continued to depend heavily upon coal liquefaction and built several plants, in total producing 3 million t/year, with the largest complex requiring 50,000 workers to produce 600,000t/year.

The price and availability of crude oil throughout most of the world since the 1950s has meant that coal liquefaction has not been economically attractive. However, in the mid 1960s in the USA there was interest in desulphurising coal to reduce environmental problems caused by the release of large amounts of sulphur oxides during coal combustion for power generation. It was thus to de-ash (and thereby reduce sulphur content) that the Solvent-Refined Coal (SRC) direct coal liquefaction process was developed, initially by the Spencer Chemical Company with an 80kg/h continuous unit funded by the Office of the Coal Research Council.

This revival of interest stimulated the preparation of a paper describing the BCURA work on solvent extraction of coal. The paper summarised three sets of laboratory-scale experiments that were carried out during the period 1955 to 1962 to examine whether a useful balance of products could be obtained economically via the solvent-extraction of low- or medium-rank coals. There had been three periods of activity: (1) from 1956, when the objective was to make available quantities of coal extract for assessment by industry, while removing the minimum amount of volatile material consistent with yielding a residue with smokeless fuel properties; (2) 1961, when the purpose was to make a similar extract by the simplest method available, to satisfy further enquiries from industry; and (3) 1962, when the objective was to test the extracts potential for conversion to jet fuel.

These experiments were conducted at atmospheric pressure, with high solvent to coal ratios (eg 10:1), and temperatures around 200°C. In some tests, ultrasonic energy was applied to promote extraction of the coal. The yield of the pitch-like extract was usually around 10% and never reached 20%. Though the experiments were not taken to the pilot scale, it was found that the residues obtained after this moderate degree of solvent extraction could be pressed into briquettes which withstood typical handling and weathering. These could be ignited readily, and burned without producing substantial smoke. The solid extracts, which had low ash and very low (<1ppm) boron contents, were considered to have potential application as binders or more probably as sources of carbon for graphite manufacture. It appeared that these carbon artifacts might be produced at little more than their fuel value. Using the simple hydrogenation equipment then available (limiting conditions to a maximum of 500°C and 300 bar) and stannous sulphide or stannous chloride as catalyst, 20-30% yields (based on extract) of partially-hydrogenated cyclic hydrocarbons were obtained. While these boiled in a suitable range for use as jet fuels, the calorific value (66MJ/kg) was lower than desired.

The results of an economic assessment, for an integrated plant producing annually 250,000t of smokeless fuel and a solid extract, suggested a case could be argued for investigations to be carried out at the pilot-scale level. However, in 1967 it was decided to focus on experiments to establish the feasibility of markedly increasing the yield of extract from the 20% level.

**ELECTRODE COKE VIA THE SOLVENT-EXTRACTION PROCESS 1967-1979**  
BCURA as part of a collaborative project with NCB, initially concentrated its investigations into the solvent extraction of coal, upon the influence of operating conditions on extraction yields and product distributions. The range of variables studied included temperature, pressure, gaseous atmosphere, residence time, coal feed size, coal rank, and solvent type, and explored their impact upon engineering problems of solids separation and distillation. This information was to be obtained in the first place from batch equipment, although it was appreciated that the product yields and operating conditions would not be identical to those pertaining to a continuous-extraction process of the type which would be needed for any large-scale exploitation of the solvent-extraction process. The experiments showed that UK coals could be solvent-extracted but when a USA economic study of the SRC process was converted to the UK situation, it was evident that the process was not at that time economic in the UK; the relative cost of coal and oil in the USA was much more favourable for liquefaction than in the UK. Other factors that favoured the economic viability of the process in the US in comparison to the UK included the relatively high sulphur content of US coals, combined with the incentives to reduce atmospheric emissions - in the UK at that time it was argued that abatement of SO<sub>2</sub> emissions was unnecessary, in part as a consequence of climatic and geographic conditions that led to dispersion of chimney plumes. In the US a positive value was assigned to the high sulphur ash residues for landfill applications.

During the experimental work at BCURA, however, quantities of coal extracts were prepared under different conditions to those used in the SRC process. UK outlets for this re-constituted, de-ashed coal were sought, eg as potentially high value feedstocks for the manufacture of electrode binders and carbon fibres. Particularly encouraging was the discovery, during testing of the coal extracts at BCURA, that the properties of coke made from the coal extract compared favourably with premium-grade petroleum coke used in the manufacture of electrodes. At that time, such a grade of coke had about three times the value of coal, thus providing the basis for a potential economic process. The electrode-coke process which did not require the use of expensive hydrogen and the associated high-pressure equipment was thus developed.

Following a series of tests, culminating in a nine-cycle demonstration run, based around a 2 litre autoclave reactor, the decision was taken by the NCB-led research committee to build a 0.5/day plant at BCURA. Construction of this was scheduled to begin in February 1971 but in the event BCURA'S status as a Research Association ceased in the week before the contractors were due to start site operations at Leatherhead, and it was decided to transfer the whole project to the Coal Research Establishment (CRE) at Stoke Orchard, near Cheltenham. Virtually all of the equipment was moved and reinstalled within a few months. At the same time, W.C. Holmes and Co Ltd began construction at Stoke Orchard of the larger rig, now termed the 'extract plant'. Erection was completed during the latter half of 1971 and instrumentation and ancillary engineering aspects, carried out by NCB staff, were completed shortly afterwards. Commissioning was completed in February 1972 and coal first fed in March 1972.

During the following six years nearly 90 runs were carried out. By far the most significant was Run 45 which started on 13 January 1975 and continued for 168 days, during which time over 30t of coke were produced. In general, this was a period when the project size increased considerably, mainly due to the increased manpower needed to operate the extract plant; the team of six at BCURA increased in about a year to 24 at CRE.

Assessment of coke quality in terms of its suitability for electrode manufacture was carried out initially by Anglo Great Lakes (AGL) using 2kg samples and later on 250kg batches from the extract plant. AGL'S long experience was extremely useful but much of the assessment was empirical and based solely upon experience with petroleum cokes and, thus, possibly not applicable to coal-extract cokes.

During 1973, the Atomic Energy Research Establishment (AERE), Harwell was contracted to fabricate some 25mm- and 75mm-diameter graphite electrodes which were subsequently submitted directly to British Steel Corporation (BSC) for testing in arc-steel furnaces. These electrodes performed much better in BSC'S tests than would have been predicted by AGL (or any other graphite manufacturer) in that they had improved resistance to thermal shock compared to electrodes made with premium-grade petroleum coke. Although having a relatively high coefficient of thermal expansion, the cracks formed in the extract-coke electrodes propagated only slowly, reducing the rate of electrode degradation.

Much encouraged by these results and the economics based upon a capital costing carried out under contract by Kelloggs, plans were made to make enough coke to fabricate 300mm-diameter electrodes that could be tested by BSC on production arc-steel furnaces. This required the extract

plant to run continuously for six months. To improve the project's ability to assess the coal-extract coke, facilities were set up at Stoke Orchard to produce and test small-diameter graphite rods. Samples of coal-extract cokes were assessed under a collaborative agreement with SIGRI (Germany) and a new agreement was negotiated with AGL. AGL used 20t of calcined extract coke supplied by NCB to fabricate 300mm-diameter graphite electrodes. The NCB graphite electrodes were vigorously tested at the Craignek works of BSC and normal production levels were maintained throughout the test period. It was concluded that coal-extract coke should be suitable for manufacture of electrodes up to and including 610mm-diameter, the largest in use at the time.

New designs and costings of larger plants, based upon specifications produced by the project, were obtained in 1977 from Catalytic Inc. However, the market for electrode coke was shrinking due to the severe contraction of the steel industry, particularly in Europe. Furthermore Conoco, at Immingham, were producing 200,000t/year of coke and Phillips, at Moerdyk in the Netherlands, were about to bring on-stream another premium-grade coke plant using a new feedstock, ethylene cracker tar. This new product also had problems getting market acceptance.

Much had been learnt about the various unit operations that made up the coal-to-electrode coke process. This was invaluable in the development of a process to produce transport fuels from coal when interest in this reemerged because of world crises in crude oil supply in the mid-1970s.

### **TRANSPORT FUELS FROM COAL-THE LIQUID SOLVENT EXTRACTION (LSE) PROCESS 1973-1986.**

The first coal hydrogenation studies in the UK since the 1960s at BCURA began in June 1973 using a 2 litre autoclave. At this time, a number of factors were threatening world crude oil supplies and the possibility of meeting at least a portion of the UK demand by synthesising oil from UK coal was considered strategically desirable. The extract plant sited at CRE was capable of supplying various streams which could have been hydrogenated (or pyrolysed) to liquids of which coal solution (the filtrate from the coal digest) and coal extract (evaporated filtrate, a solid at room temperature) were favoured technically because:

- they contain little inorganic material to contaminate catalysts and cause blockages in the plant
- the relatively unreactive inertinite portion of the coal has been removed
- they can be made fluid easily e.g., by the application of heat.

Coal extracts contain higher proportions of coal-derived material than coal solutions, so that changes in the coal material can be detected more readily. However, the higher softening points of coal extracts make them more difficult to pump.

The primary aim of the preliminary investigation was to hydro-treat coal extracts using the autoclave in order to explore possible process configurations and identify those with potential for development. However, the work had the additional aim of detecting possible problems at the more extreme conditions likely to be encountered during scale-up. An extra function was the production of liquid samples for evaluation as chemical feedstocks by the Dutch State Mines. This work was carried out in the period June to December 1973 and was the precursor to a substantial programme of research supported and partially funded by European Economic Community (EEC) between 1974 and 1986.

Autoclaves were the only equipment available in the first few years but by 1976 coal-extract solutions were provided to British Petroleum (BP) for tests in their continuous-hydrocracking unit (CHU). Although originally it was hoped to continue this arrangement, separation of the extraction and hydrocracking stages between two sites hindered detailed recycle experiments. Consequently, additional funding was obtained and BP built a new CHU, installed it at CRE and provided training for operators and maintenance engineers. This unit, together with associated facilities built at various times, eg extract production using a dedicated integrated solvent-extraction plant (ISEP), was the key experimental facility for the research programme. Many aspects of liquefaction, eg catalyst selection, were first studied or screened on smaller equipment but the aim was always to confirm potential process improvements in recycle runs on the CHU-ISEP equipment [or the Integrated Liquefaction Plan (ILP) as it was renamed in 1983].

The main criteria by which success during repeated recycling was gauged were that 100% recovery of solvent was achieved, that the power of the solvent to dissolve the coal remained adequate and that pitch-plus-filter cake represented no more than 40wt% (dmmf) of the coal. Solvent quality during repeated recycling demanded much attention; obtaining the balance between hydrocracking (of the extract) and hydrogenation (of the solvent) proved to be particularly difficult. However, solutions to all the problem areas were found and in 1984 what was deemed a totally successful run was carried out.

During the period 1977-1986, over 30,000h running of the ILP were achieved with nearly 6000h in 1984. Such long periods of operation were essential to prove catalyst life. Mass balances were carried out for virtually every day of operation and closures of over 95% became standard. The complexity of the plant, plus the amount of handling necessary to take the many samples that

were needed to assist interpretation, meant that these good balances were only achieved by continued vigilance by operators and supervisors. The success of the ILP programme owed much to the teamwork of the over 30 people involved. In addition to the studies supporting the ILP programme, much work was carried out during this period on the various unit operations, particularly on filtration using both small- and large-scale equipment (eg the extract plant in which other filters were installed). Secondary refining facilities were constructed with which finished gasolines and diesels were prepared, tested and also demonstrated in various vehicles (a lawnmower driven by Sir Derek Ezra, then Chairman of the NCB, a dumper truck by John Moore, Energy Minister, Automobile Association vans in the Lord Mayor of London's procession, as well as tests to measure fuel consumption, emissions, etc).

Proposals to build demonstration plants were made in the late 1970s and subsequently the siting of such a plant at Point of Ayr, North Wales, was agreed upon at an early stage. Consequently, Point of Ayr coal was chosen as the standard coal for use in experiments from 1981. Many other coals from around the world were tested on the small-scale and several in the ILP, including Illinois No. 6 coal which proved extremely easy to process. One of the major advantages of the LSE process that has emerged is its ability to handle virtually any coal regardless of rank or ash content.

The design specification for the Point of Ayr plant was based upon information obtained up to 1983. Many configurations were considered and four incorporated into the design, ie

- single-stage hydrocracking
- two-stage parallel hydrotreatment
- two-stage series hydrotreatment
- pitch recycle to hydrocracking

#### LSE PROCESS DEVELOPMENT PILOT PLANT, POINT OF AYR 1980-1992.

During the mid-1970s there were proposals to build larger electrode-coke plants, and these were considered in the Coal Industry Examination carried out in 1974. Its terms of reference were: *"To consider and advise on the contribution which coal can best make to the Country's energy requirements and the steps needed to secure that contribution"*.

With regard to the LSE project at the time, to quote the report: *"The NCB have pointed out that the prime objective of the project is the development of a liquid fuel from coal process, and that whilst the economics of electrode-coke production look attractive, the market is limited and a commercial venture could not carry the cost of developing the whole process. The extract hydrogenation stage provides the bridge to lighter hydrocarbon liquids, both fuels and chemical feedstocks, but this is still in the laboratory stage"*.

The report concluded: *"We consider that the combination of NCB expertise, relevance to the UK economy, and commercial prospects, justifies concentration on three areas, fluidised bed combustion, coal liquefaction by solvent extraction and pyrolysis"*.

Support came relatively quickly for the fluidised bed combustion project (at Grimethorpe, UK) but it was some time before an acceptable pilot plant project for the LSE process was formulated. However, in 1980 Matthew Hall Ortech (MHO) were chosen as contractors to perform design and costings of 25t/day pilot plants comprising LSE and supercritical-gas extraction (SGE) front-ends with a common hydrocracking facility. SGE was abandoned soon after in 1982, partly as a result of MHO's reservations about further scale-up of this process.

However, the LSE 25t/day plant plan did not receive UK Government support. In late 1982, ICI were called in by the Chief Scientist at the Department of Energy as consultant to advise on the scale of the development proposed by the NCB. ICI in their 'audit' proposed that engineering information could be obtained at a scale of 1t/day; NCB continued to consider that 25t/day was necessary on the basis of the process information that had been produced at CRE. However, in order to proceed, a compromise was reached in which a throughput of 2.5t/day was agreed (the base case in the specification, therefore, was 100kg/h of dry, mineral matter-free coal).

The EEC had always been highly supportive and initial approval to provide significant funding for the 25t/day plant had been granted but had to be cancelled. The UK Government stipulated that to receive their support for the 2.5t/day plant, EEC funding had also to be obtained, project management should be strengthened and at least one private company should participate. Oil company support was not forthcoming for various reasons. However, this impasse was finally resolved by an agreement between Ian McGregor (Chairman of NCB) and Peter Walker (Secretary of State for Energy) in which funding from the Department of Energy and the EEC was released on the understanding that the NCB would make every endeavour to find a commercial partner. (This was eventually achieved when Ruhrkohle Oel und Gas GmbH and Amoco Corporation joined the Project in 1987 and 1991, respectively.)

A steering committee was responsible for the project and it set the following objectives:

*"The next stage in the development of the NCB's Liquid Solvent Extraction (LSE) process is to*

*design, build and operate a 2.5t/day Process Development Pilot Plant (PDPP).*

*The primary objective is to demonstrate that the LSE process can be operated continuously using solvent derived from the feed coal; this requires that solvent quality and quantity be satisfactorily maintained and controlled and satisfactory yield pattern of distillates obtained.*

The project was nominally separated into four phases, ie specification, construction, commissioning and operation, and each phase was contracted separately. During the first phase, funded by the Department of Energy and BCC (the successor to NCB), the overall project costs and scheduling were ascertained. Following this, the complete project was approved in October 1985 by BCC's Board and agreements reached with the Department of Energy and the EEC.

There were contractual and other problems during the construction phase which delayed commissioning and the planned recruitment, and the full project operating time was rephased accordingly. However, the delay at Point of Ayr provided the opportunity to review again all aspects of the process and as a result additional experimental projects were proposed with separate funding arranged with the European Coal and Steel Community (ECSC) and BCC. This made particularly good use of CRE staff who were to form the core of the Point of Ayr staff and significant advances in certain areas were made.

In addition to the CRE experimental work, studies have also been made on economic aspects. This included a commercial plant design and costing performed by Costain Ltd. The design reflected the evolved LSE process and the costing procedure enabled variations in the process (eg when using different coals) to be estimated with some confidence. The objective of this particular study was two-fold. In addition to giving up-to-date economic figures, it was intended to guide the Point of Ayr plant's operating programme such that the variables studied were those that could have the biggest economic impact rather than those which were academically perhaps more interesting.

Another study commissioned in 1991 was to consider how coal liquefaction might be introduced into the European refinery scene. This required the contractor, Trichem Consultants Ltd, first to predict the future European oil refinery situation well into the next century and then to estimate the value to refiners of coal-derived liquids.

A way of expressing the process economics is to calculate what the price of crude oil has to be for a coal liquefaction plant to give a nominal internal rate of return, eg 10%. Currently, this 'break-even oil price' is around \$35/bbl (for coal priced at \$60/t) although this could be reduced in several ways. For example, if the coal price was reduced to \$20/t, the break-even oil price could be as low as \$25/bbl. Clearly, a liquefaction plant located near a cheap source of coal would seem to be a good solution. Unfortunately, most locations of cheap coal are such that the plant construction costs would be much higher (than for the base-case coastal location) and no net benefit would accrue. Consequently, the search for the ideal combination of cheap coal and cheap plant construction costs continues.

## CONCLUSIONS

Direct liquefaction technology in the UK has advanced considerably from the stage in 1967, when little was known of the way in which UK coals behaved. Work on the electrode coke process not only extended knowledge of liquid solvent-extraction of coals but also showed conclusively that coal-based carbon materials were technically feasible and could be produced commercially. The LSE process, extended the first development to show that petrol and diesel fuels could be produced with high efficiency, not only from UK coals but also from essentially any coal worldwide.

Knowledge accumulated from developing and proving these processes has been achieved through the efforts of many individuals and organisations, including those who ensured the availability of funds, those who were creative in overcoming problems and those who engineered the solutions. The key benefit of all these contributions and developments is that UK liquefaction technology has been advanced to the point that when, as it eventually will, the price of oil rises, action can be taken to enable coal to provide a realistic, alternative source for transport fuels.

## REFERENCE

(1) G.M. Kimber, "A History of U.K. Coal Liquefaction" COAL, R078, ETSU, Harwell, U.K., Dec. 1996.

# RECENT ADVANCES AND FUTURE PROSPECTS FOR DIRECT COAL LIQUEFACTION PROCESS DEVELOPMENT

F. P. Burke and R. A. Winschel  
CONSOL Inc.  
Research & Development  
4000 Brownsville Road  
Library, PA 15129

David Gray  
Mitretek Systems  
7718 Old Springhouse  
McLean, VA 22102-3481

Keywords: Direct Liquefaction, Process Development, Economics

## ABSTRACT

Over the last fifteen years, the technology for the direct conversion of coal to liquid fuels has undergone significant development. This has been most evident in improvements in product yields (i.e., barrels per ton of coal), product quality, and, ultimately, in projected product costs. These advances have occurred through the optimization of process conditions and, particularly, a better understanding of the selection and use of catalysts. In addition, engineering and economic evaluations of the liquefaction process alternatives, and macroscopic analysis of global fuel production and consumption have been essential in guiding process development and providing a justification for investment in further R&D. This paper will highlight some of the important technical achievements in reaching the current state of direct liquefaction process development, and provide some speculation on the opportunities and obstacles for future research and commercial implementation.

## THE WORLD AND UNITED STATES OIL SITUATION

Petroleum use worldwide is about 65 million barrels per day (MMBPD), and the Energy Information Administration (EIA) predicts that by 2015, worldwide demand will increase to between 89 and 99 MMBPD.<sup>1</sup> Over 55% of world petroleum is used in the transportation sector. Liquid hydrocarbon fuels are ideal for transportation since they are convenient, have high energy density, and a vast infrastructure for production, distribution and end use is already in place. The estimated ultimate world resource of oil and natural gas liquids (NGL) is 2.5 trillion barrels; the sum of 1.2 trillion barrels for OPEC and 1.3 trillion barrels for non-OPEC.<sup>1</sup> Estimates of proven reserves of oil vary over time because more of the oil resource moves into the reserve category as a result of variations in the world oil price (WOP) and available technologies. However, the estimated ultimately recoverable world conventional oil resource (EUR) has been remarkably similar for the last 25 years. James MacKenzie of the World Resources Institute<sup>2</sup> cites an analysis of 40 estimates of ultimately recoverable oil, for the years 1975 to 1993, conducted by David Woodward of the Abu Dhabi Oil company. In this analysis, Woodward concluded that "there is a fair degree of consistency among the estimates with the average being 2,000 billion barrels (BBO) and 70% falling in the range of 2,000 to 2,400 BBO."

Mitretek has performed analyses of world oil demand and potential supply from the present until 2100.<sup>3</sup> The results of these analyses show that when the projected world oil demand is plotted on the ultimate resource curve whose integral is equal to 2.5 trillion barrels, it becomes clear that conventional world oil production will peak in a timeframe from about 2015 to 2020 and then irreversibly decline because of resource limitations.

Because oil is the primary fuel in the transportation sector, Mitretek also examined the potential impact of the above world oil supply scenario on the U.S. transportation sector.<sup>3</sup> This analysis concludes that, even with a rapid penetration schedule for alternatively fueled vehicles, there is likely to be a significant shortfall in petroleum supply in the United States before 2015.

## THE DEVELOPMENT OF DIRECT COAL LIQUEFACTION TECHNOLOGY

Direct coal liquefaction is the process by which coal is converted to liquids through the addition of hydrogen or the removal of carbon. Hydrogen can be provided directly from the gas phase, through transfer from a chemical source such as a hydrogen donor, or carbon can be removed by a disproportionation reaction in which the coal is converted to (relatively) hydrogen-rich and carbon-rich products. The reaction generally requires temperatures above the softening point of coal (typically around 600 K) to facilitate mass transport and to achieve adequate rates of reaction. Although liquids of some description can be produced by a number of approaches, the objective usually is to produce

transportation grade fuels as substitutes for petroleum-derived gasoline or diesel fuel. The reactions involved include hydrogenation and cracking, and removal of nitrogen, oxygen and sulfur from the coal (primarily as  $\text{NH}_3$ ,  $\text{CO}$ ,  $\text{CO}_2$ ,  $\text{H}_2\text{O}$ , and  $\text{H}_2\text{S}$ ). The mechanisms of these reactions generally involve both hydrogenation and bond cleavage, although opinions differ as to the reaction sequence.

The cost of producing coal liquids is implicit in these chemical reactions. There is a theoretical minimum amount of hydrogen that is necessary to convert the (empirical) coal structure to liquid products of some specified composition. In practice, the amount of hydrogen consumed (typically 6-7 wt % on a moisture-ash-free coal basis) will be greater than the theoretical minimum because of undesirable side reactions, such as methanation of carbon oxides and  $\text{C}_1$ - $\text{C}_4$  gas formation due to cracking. Because hydrogen is expensive, there is a strong incentive to minimize its consumption, but the quality of the product liquid must be known for a comparison of hydrogen consumption values to be meaningful.

The liquefaction reactions require elevated temperatures to proceed at reasonable rates; this requires some pressure containment (~500 psig) to keep the reactants in the liquid phase. If molecular hydrogen is used as the hydrogen source, higher operating pressure (2000-3000 psig) is required for adequate mass transfer. The combination of elevated pressure and temperature is an important factor in determining the capital cost of the liquefaction train, including heat-transfer units, reactors, pumps, pressure let-down systems, etc. Effective catalysts can decrease both the reaction pressure and temperature. Given the heterogeneous nature of coal, the presence of mineral matter, and the variety of functional groups present, it is likely that some form of catalysis occurs, even if an external catalyst is not used. In fact, catalysts are universally employed in practical liquefaction processes, with solid heterogeneous catalysts being the most common. Historically, the first commercial liquefaction plants in Germany used the I. G. Farben process, in which coal was liquefied at 760 K and 10,000 psig in a liquid phase reactor using a relatively inactive iron catalyst. Because of the reaction severity, the German plants produced high hydrocarbon gas yields (30 wt % MAF coal) with a correspondingly high hydrogen consumption (~14 wt % MAF coal).

In the United States, the development of direct liquefaction technology was stimulated by the petroleum shortfalls and price increases of the 1970s. By 1980, three process concepts (SRC-II, EDS and H-Coal) had been sufficiently advanced to merit consideration for commercialization. An interest in producing a substitute fuel oil for electric utility boilers led the Southern Company and Electric Power Research Institute to explore the Solvent Refined Coal (SRC) process on the 6 tpd Wilsonville, Alabama facility. This was a one-stage thermal process in which coal was solubilized in a recycle solvent, and the product was deashed to remove mineral matter and some sulfur. A variant of this was the SRC-II process, developed by Gulf Oil Company and others. In the SRC-II process, coal was hydrogenated in a one-stage reactor with no catalyst addition, but the distillation bottoms were recycled to take advantage of the catalytic activity of the coal mineral matter. The SRC-II process was piloted on a 50 tpd unit at Ft. Lewis, WA. The Exxon Donor Solvent (EDS) process was developed through the 250 tpd pilot plant scale at Baytown, TX. In the EDS process, the coal was fed to a plug-flow reactor in a recycle solvent (the donor solvent) that was hydrogenated catalytically in an external reactor. The donor solvent provided the hydrogen for the liquefaction reaction. In later development, a bottoms recycle stream was added to the EDS feed to provide additional residence time for conversion, and perhaps to utilize the catalytic activity of the mineral matter. One common feature of these processes, and others such as the CONSOL CSF process and the British Coal LSE process, was that the primary coal liquefaction reactions took place in the absence of any added catalyst, ostensibly to avoid the rapid deactivation of the catalyst that was presumed to occur in the presence of the coal mineral matter.

In the HRI H-Coal process, the issue of catalyst deactivation was addressed by utilizing an ebullated bed reactor which allowed a supported catalyst to be added and withdrawn continuously. The ebullated bed reactor also offered superior performance in terms of heat and mass transfer. The H-Coal process was developed at HRI's bench-scale and PDU facilities in Lawrenceville, NJ, and piloted on a 250 tpd unit in Catlettsburg, KY. Representative operating conditions and yields for the H-Coal pilot plant operations with Illinois basin bituminous coal are shown in Table 1. The process made a relatively light product (proportion of naphtha) but also had a sizeable yield of hydrocarbon gases and unconverted resid, which reduced overall liquid yield.

One problem with the single catalytic stage is that hydrogenation reactions are best done at relatively low temperatures where the equilibrium is more favorable, but conversion

(i.e., cracking) reactions are faster at higher temperature. To overcome this, research was conducted on the use of multiple reaction stages, exemplified by work by Lummus and Cities Service in New Brunswick, NJ. In the Lummus/Cities bench unit, the coal was converted to a soluble form in the first stage at relatively high temperature (~720 K) but short contact time (~2 min). The first-stage product was deashed, and converted to distillate liquids at around 670 K in an ebullated bed LC-Finer unit, which simultaneously produced a hydrogenated solvent for recycle to the first stage. A similar configuration was installed at the Wilsonville SRC pilot plant, which employed a Kerr-McGee Critical Solvent Deasher between a thermal first stage and an ebullated bed second stage supplied by HRI.

Lummus first recognized, and Wilsonville later confirmed, that the location of the deashing unit between the two stages had little effect on catalyst life. The most important factor in catalyst deactivation was carbon laydown, not poisoning by metals in the mineral matter. This led to "close coupling" of the two reactor stages, with deashing applied to the second-stage product. It also allowed for "ashy recycle", in which a portion of the second-stage product is recycled directly to the first stage. By concentrating solids in the recycle stream, the amount of material processed by the deasher was significantly reduced, and the unconverted coal was given additional residence time. The Wilsonville unit subsequently was used to explore a variety of staged reactor configurations, including two ebullated bed catalyst stages ("catalytic/catalytic" mode), the use of a dispersed iron oxide as a first-stage catalyst with subbituminous coals ("thermal/catalytic" mode), and alternative temperature staging. As shown in Table 1, this resulted in substantial reductions in hydrocarbon gas and resid production for bituminous coal, with a corresponding increase in distillate liquids, although the product was higher boiling than that of the H-Coal process. Results with subbituminous coal (Table 2) were similar, although a high first-stage temperature was still required to achieve adequate coal conversion. One advantage of the "thermal" first stage is a greater removal of oxygen as carbon oxides. In the single-stage system, carbon oxides are converted catalytically to methane and water, with increased hydrogen consumption.

Although the first stage in the thermal/catalytic mode did not contain a supported catalyst, the Wilsonville unit was fed a powered iron oxide catalyst to promote coal conversion. This was consistent with research at Mobil R&D showing that solid catalysts promote the conversion of coal to soluble forms. Subsequent work at Wilsonville, HRI, and a number of academic institutions explored the use of dispersed catalysts based on iron, molybdenum, and other metals. In a current collaborative project, CONSOL, the University of Kentucky, LDP Associates, Hydrocarbon Technologies Inc. (HTI), and Sandia National Laboratories have been exploring several advanced concepts for improving direct liquefaction process economics through modifications to the feed coal and recycle solvent and the use of dispersed and impregnated slurry catalysts. This work has progressed through laboratory studies to evaluation of the process concepts in bench-scale continuous unit runs at HTI, the former experimental facilities of HRI. The first run (ALC-1) was made in the all-slurry catalyst mode with molybdenum and iron catalysts. Potential advantages of operation with all-slurry catalysts include: simplified reactor design; simplified operations, constant catalyst activity, more efficient use of reactor volume (no volume needed for catalyst support); and catalyst can be recycled with solids to reduce the fresh catalyst requirements. Raw subbituminous coal was used in condition 1 of Run ALC-1; the same coal cleaned by oil agglomeration was fed in condition 4 (Table 2). In condition 5 (not shown in Table 2), the distillate portion of the recycle solvent was dewaxed and hydrogenated to improve solvent quality. As shown in Table 2, these operations produced exceptional distillate yields of 66% to 69% MAF from subbituminous coal. This was accomplished by near-extinction conversion of residual oils, including unconverted coal. The somewhat higher hydrogen consumptions in these operations resulted, in part, from the higher gas yields due to the higher reaction temperatures, but they also resulted from the use of an in-line gas-phase hydrotreater for the distillate product. These operations produced a low-heteroatom, highly hydrogenated product with low boiling point.

## OPPORTUNITIES FOR FUTURE RESEARCH AND DEVELOPMENT

As summarized above, the analysis by Mitretek indicates that the time when worldwide petroleum demand begins to deplete resources may come within the next two decades, even without significant political or economic disruptions. Therefore, it is essential simultaneously to pursue a number of options to mitigate the future shortfall in domestic petroleum. These options are: to continue domestic exploration and production using the best technologies available, to continue to develop and deploy alternatively fueled vehicles, and to continue to improve efficiencies in all sectors of transportation. Yet, even with these steps, this analysis indicates that the domestic demand for liquid fuels will exceed our potential sources of supply. Continuing our reliance on oil imports to alleviate the shortfall is not a long-term solution. Rapidly increasing world oil demand will put ever-increasing pressure on the oil supply and the WOP will rise. The inevitable conclusion is that

additional options will be necessary to ensure that the United States will have the necessary liquid fuels supply to be able to continue economic growth into the 21st century. One of these additional options is to produce liquid fuels from our huge domestic coal resources.

Current direct coal liquefaction technology is technically feasible, but not economically competitive. However, with world oil prices over \$25/bbl at this writing, it is clear that, in the long term, the upward pressure on oil prices persists. Research should be directed toward reducing the cost of liquid products so that these alternative technologies are available as early as possible to have the greatest economic benefit. Several technical issues are pertinent to achieving that objective.

**Catalysts.** Despite all the research that has been done on catalyst development and testing, improved catalysts still offer the single best opportunity for affecting many of the cost features in a liquefaction process, including yields, selectivity, product quality, hydrogen utilization, and capital cost (through reduced pressure and temperature and increased space velocity). A problem with much catalyst research is that it is done at unrealistic conditions, with results that are not easily translated to a process context. For example, identifying a catalyst that improves coal conversion from 40% to 60% is of little value when the process goal is produce specification products at high yield. On the other hand, identifying a truly improved catalyst could open significant opportunities for redefinition of the basic process concept.

**Feedstock Selection.** The principal feedstocks are coal and hydrogen. Most coals have been shown to be suitable for most processes. If there is an "opportunity" coal, it will be the result of economic opportunity; for example, the current emphasis on U.S. low-rank coal recognizes its low mine-mouth cost. Reduction in hydrogen cost is problematic. Production of hydrogen from coal involves a large unavoidable capital expenditure for the gasification plant. Production from natural gas is unlikely to be economical in the long term, particularly if petroleum prices have risen. Coprocessing feedstocks, such as waste plastics and heavy resid, may be useful in providing an economic justification for early "pioneer" plants which will demonstrate commercial viability.

**New Reaction Mechanisms.** Despite its variations, current liquefaction technology remains based in the early German technology, i.e., thermal free radical or radical-initiated hydrogen transfer. There are other possible hydrogen transfer chemistries, including carbonium ion, hydride ion and biochemical mechanisms. Although these have been explored, they have yet to yield a promising candidate. As with the catalyst research, much of the problem may lie in a failure to establish exploratory research goals of such a nature that they can be used to justify further development. A realistic candidate must be able to achieve high yields of liquids that meet some minimum standard of quality or upgradability.

#### REFERENCES

1. Annual Energy Outlook 1996 With Projections To 2015. Energy Information Administration, January 1996. DOE/EIA-03893 (96).
2. MacKenzie, James J. *Oil as a Finite Resource: When is Global Production Likely to Peak?* Paper from the World Resources Institute, March 1996.
3. Gray, David, and Glen Tomlinson, *Rationale and Proposed Strategy for Commercial Deployment of Coal-Derived Transportation Fuels*, Mitretek Report MP 96W0000209, June 1996.

TABLE 1

OPERATING CONDITIONS AND YIELDS FOR H-COAL, ITSL, AND CMSL,  
ILLINOIS BASIN COAL

	H-Coal Pilot Plant Run 8	ITSL Wilsonville Run 252B1	ITSL Wilsonville Run 257J	CMSL HTI Run PB-05/2
Year	1981	1987	1989	1996
<b>Conditions</b>				
<u>Stage 1</u>				
T, K	728	705	705	720
H <sub>2</sub> Partial pressure, psi, inlet	2500	2500	2600	2500*
Catalyst age, lb coal/lb	1690	-1300	645	Dispersed
S.V., lb coal/hr/ft <sup>3</sup> reactor, each stage	29	-	-	42
<u>Stage 2</u>				
T, K	None	672	678	731
Catalyst age, lb coal/lb	None	-470	1309	Dispersed
<b>Yields, wt % MAF</b>				
H <sub>2</sub> O	7.5	9.6	10.2	4.3
H <sub>2</sub> S, NH <sub>3</sub> , COx	3.8	5.1	5.0	6.1
C, x C <sub>2</sub> Gas	12.8	6.5	5.4	6.7
Naphtha	22.9	17.5	14.5	18.4
Middle Distillate	20.0	7.8	7.1	16.0
Gas Oil	7.6	44.1	44.2	39.0
Total Distillate	50.5	69.4	65.8	73.4
Resid	31.3	16.4	19.7	14.8
H <sub>2</sub>	-6.0	-7.1	-6.0	-5.2
Coal Conversion	96.1	93.0	91.7	96.2

\*Unit back-pressure

TABLE 2

OPERATING CONDITIONS AND YIELDS FOR H-COAL, ITSL, AND CMSL,  
POWDER RIVER BASIN COAL

	H-Coal PDU Run 10	ITSL Wilsonville Run 262D	CMSL HTI Run ALC-1/1	CMSL HTI Run ALC-1/4
Year	1980	1991	1996	1996
<b>Conditions</b>				
<u>Stage 1</u>				
T, K	719	713	715	716
H <sub>2</sub> Partial pressure, psi, inlet	2500	2800	2500*	2500*
Catalyst age, lb coal/lb	742	Dispersed	Dispersed	Dispersed
S.V., lb coal/hr/ft <sup>3</sup> reactor, each stage	25	-	42	26
<u>Stage 2</u>				
T, K	None	694	726	726
Catalyst age, lb coal/lb	None	727	Dispersed	Dispersed
<b>Yields, wt % MAF</b>				
H <sub>2</sub> O	16.3	13.9	13.8	16.2
H <sub>2</sub> S, NH <sub>3</sub> , COx	3.5	6.7	5.9	5.1
C, x C <sub>2</sub> Gas	11.0	5.3	9.4	12.4
Naphtha	24.3	12.9	18.6	23.0
Middle Distillate	14.5	7.7	11.3	9.7
Gas Oil	11.9	40.1	39.2	33.4
Total Distillate	50.7	60.8	69.0	66.1
Resid	24.1	18.7	9.4	7.1
H <sub>2</sub>	-5.6	-5.5	-7.5	-8.8
Coal Conversion	91.0	90.1	95.0**	97.5**

\*Unit back pressure

\*\*SO<sub>2</sub>-free ash basis

# COAL PHOTOLUMINESCENCE: MODIFICATION OF SURFACE PROPERTIES AND GEOCHEMICAL AND TECHNOLOGICAL IMPLICATIONS

Alan Davis and Gareth D. Mitchell

Coal & Organic Petrology Laboratories, Department of Geosciences,  
105 Academic Projects, Penn State University, University Park, PA 16802

**Keywords:** coal luminescence, coal fluorescence, coal hydrophobicity

## INTRODUCTION

The luminescence behavior displayed by vitrinite across the coal rank range upon exposure to microscopic blue- and UV-light irradiation, has been explained by Lin et al. (1) using the molecular-phase concept. Two peaks occur in the trend of vitrinite luminescence intensity with rank. The first of these, at the low maturity end of the series represented by peats and lignites, displays the highest intensity levels. This "primary fluorescence," is considered to be due to the presence of lignin-derived structures (2); it is almost eliminated by about the subbituminous C/B boundary owing to the progressive luminescence quenching which accompanies condensation. It is the second peak, centered at high volatile A bituminous rank (reflectance of about 0.9%), which Lin et al. have attributed to the development of the mobile or molecular phase within the vitrinite. The same coals give the highest yields of chloroform solubles. It is these extractable components which are responsible for the luminescence response of the vitrinites; whereas the aromatic and polar fractions of hexane solubles were highly luminescent, the chloroform-extracted residue of mildly pre-heated vitrinite was not visibly luminescent. This residue is considered to represent the aromatic network which is too highly condensed to luminesce in bituminous coals; delocalization of electrons in the macromolecules within this rank range causes intense quenching.

With increasing time of exposure to UV or blue light under an air objective, the luminescence intensity displayed by vitrinite undergoes progressive or variable changes in patterns which are rank dependent. Davis et al. (3) have shown that this phenomenon, termed "alteration", results mainly from photochemical oxidation; it does not occur when an inert medium is used instead of air. A cationic dye, Safranin O, which is sensitive to oxidized coal surfaces, responds positively to the air-irradiated surfaces. FTIR spectroscopy reveals that a major change resulting from the air irradiation is an increase in carbonyl functional groups.

One purpose of this paper is to review some of the geochemical factors, in addition to rank, which influence the luminescence response of vitrinite. Another is to discuss how the molecular-phase concept has been applied to the results of quantitative luminescence photometry of the products of dry, catalytic hydrogenation. However, most of the results reported here are concerned with an investigation of the relationship between oxygen functionality and hydrophobicity. Advantage has been taken of the photo-oxidation technique to modify the surface chemistry of vitrinites so that variation in contact angle and floatability can be related to specific changes in FTIR-determined oxygen functionality.

## INFLUENCE OF DEPOSITIONAL ENVIRONMENT UPON VITRINITE LUMINESCENCE

Although rank has a dominant influence in determining the luminescence behavior of coals, there is also some influence exerted by the depositional environment. Several investigators have observed higher luminescence intensities displayed by vitrinites deposited in a marine-influenced environment compared to those not so influenced. Rathbone and Davis (4) reported a positive correlation between luminescence intensity and total sulfur of an iso-rank series of bituminous coals; they discussed the possibility that the phenomenon might be related indirectly to a greater incorporation of bacteria-derived lipids into coals deposited in a marine setting. Zhang et al. (5) have suggested an alternative mechanism through which sulfur-linked aliphatic structural units acquired during early coalification has directly enhanced vitrinite luminescence intensity. Py-gc/ms and solid-state  $^{13}\text{C}$  nmr of vitrinites and luminescence measurements on model compounds led to the conclusion that bacterially reduced sulfur species can vulcanize functionized lipids onto the macromolecular phase. In contrast, increased levels of phenolic compounds present in low-sulfur freshwater vitrinites are associated with lower luminescence intensities.

## LUMINESCENCE PHOTOMETRY OF LIQUEFACTION RESIDUES

Quantitative luminescence photometry was one technique used to interpret the structural changes involved during dry, catalytic hydrogenation (6,7). Measurements were taken on the unextracted

liquefaction products and on the subsequent extracts. For example, hydrogenation experiments were performed using a high volatile bituminous coal and an impregnated molybdenum catalyst at 400°C for four different reaction times. The absence of a liquid vehicle is essential so that the liquid products are not removed from the coal. With increase in time up to 60 min, the luminescence intensity of the unextracted residues increased progressively and markedly from the zero reading obtained with the fresh coal. This increase closely paralleled the proportion of chloroform extracts obtained from the series of hydrogenated coals, a correspondence suggesting that the luminescence is a response from relatively low molecular weight materials representing both the molecular phase of the coal and products from the breakdown of the network. Indeed, the luminescence of the vitrinite residue, induced by hydrogenation, showed a red shift (increase in wavelength) as hydrogenation temperature was increased from 350 to 400°C; this shift is consistent with the increased generation of asphaltenic materials from the network. The chloroform extract of the 400°C residue was highly luminescent (the residue was not); two physically distinct components were recognizable. The component with by far the highest luminescence intensity had a spectral peak wavelength corresponding to that of the oil (hexane-soluble) fraction of the hydrogenation products, whereas that of the less luminescent component had a spectral peak corresponding to that of the asphaltene fraction.

#### PHOTO-OXIDATION AND HYDROPHOBICITY OF BITUMINOUS COALS

Severe oxidative weathering has a negative influence on the behavior of coals in most industrial processes including cleaning. As coals are increasingly oxidized they become less hydrophobic and more difficult to separate from mineral matter by flotation.

The surface photo-oxidation of bituminous coals which occurs as a result of blue- and UV-light irradiation shares many similarities with naturally weathered coal. Therefore, light of 390-490 nm has been used to prepare oxidized vitrain surfaces. These have been employed in experiments to establish correlations among surface oxygen functionality, surface hydrophobicity, flotation yield and, as a readily measurable index of oxidation, luminescence intensity.

An optical microscope was used to measure luminescence intensity (in N<sub>2</sub>) and alteration (in air), and to photo-oxidize freshly polished surfaces of vitrains collected from a suite of coals of varying bituminous rank (hvCb to mvb) using a blue-light flux. Irradiations were conducted for 0, 1, 5 and 10 mins. The change in near-surface chemical functionality was measured using reflectance-mode FTIR. Contact-angle measurements were made on these same irradiated surfaces to obtain a correlation among chemical changes, luminescence intensity and wettability.

Scribe marks were cut perpendicularly across selected vitrain bands on polished blocks of coal, and successive 200µm diameter areas were irradiated in two adjacent lines parallel to each mark to create 0.4mm wide oxidized zones. During the course of the irradiations, photometric readings were obtained of the change in luminescence intensity with time (alteration).

A sessile drop technique was used to determine the change in surface wettability. Using a syringe and micro-pump, a drop of distilled water was advanced from the fresh vitrain surface across the photo-oxidized area and contact angles measured at regular intervals. These same areas were subsequently relocated for measurement of variation in functional group chemistry using reflectance-mode FTIR.

A comparison of the luminescence, contact angle and FTIR spectra for the fresh and varying ly photo-oxidized vitrain surfaces for three of the coals studied is given in Figures 1 and 2. Luminescence intensity changes characteristically during irradiation in air; for fresh bituminous coals there is either a negative (intensity decrease) or dual (decrease followed by increase) response, depending upon coal rank (first column, Figure 1). The reflectance FTIR spectra (Figure 2) show a progressive increase in absorbance in the carbonyl region (~1775-1650 cm<sup>-1</sup>) and a decrease in the aliphatic region (~3030-2850 cm<sup>-1</sup>) with irradiation time. The spectra also suggest that the O-H region near 3450 cm<sup>-1</sup> may increase upon irradiation. Considering these results, the influence of photo-oxidation on surface wettability (second column, Figure 1) is predictable, i.e., the magnitude of change in contact angle increases with irradiation time. These effects decrease with rank.

The results suggest that the luminophores on the surface of fresh bituminous coals are initially quenched by oxygen, causing a decrease in emission intensity, with only marginal influence upon

near-surface chemistry and wettability. However, with increasing exposure, an increase in the spectral region occupied by ketones, aldehydes and esters suggests a variety of reactions involving carboxylic acid groups and anhydrides that would affect the intensity of luminescence alteration.

#### CONCLUSIONS

Rank is the dominant influence in determining the luminescence behaviors of coals; however, measurable effects representing the depositional environment can also be encountered. In marine-influenced environments, lipoidal material may have become incorporated into the coal precursor molecule through a sulfidization process, leading to an enhancement of luminescence intensity.

The results of quantitative luminescence spectrometry support the conclusion that the more intense levels of coal hydrogenation in a series of dry, catalytic experiments were achieved by disruption of the macromolecular network and the production of asphaltenes.

Blue-light irradiation using photometric microscopy provides a means of progressively oxidizing the surfaces of vitrains. The reflectance FTIR measurement on irradiated areas shows an increase in the carbonyl and decrease in aliphatic regions that are similar to results observed in laboratory and natural oxidation studies. The changes in infrared spectra and wettability are more pronounced with increasing radiation time and with lower rank. Some contribution to the oxidation of coals exposed at the face of strip mines and in stockpiles may have arisen as a result of exposure to the ultraviolet irradiation of sunlight.

#### ACKNOWLEDGEMENTS

The authors gratefully acknowledge the financial support of U.S. Dep. Energy Grant No. DE-FG22-93PC93223. Much of the work referenced was undertaken in collaboration with past and present colleagues within the College of Earth and Mineral Sciences at Penn State.

#### REFERENCES

1. Lin, R., Davis, A., Bensley, D.F. and Derbyshire, F.J., *Internat. J. Coal Geol.*, 6, 215 (1986).
2. Stout, S.A. and Bensley, D.F., *Internat. J. Coal Geol.*, 7, 119 (1987).
3. Davis, A., Rathbone, R.F., Lin, R. and Quick, J.C., *Org. Geochem.*, 16, 897 (1990).
4. Rathbone, R.F. and Davis, A., *Org. Geochem.*, 20, 177 (1993).
5. Zhang, E., Mitchell, G. D., Davis, A. and Hatcher, P.G., *ACS Div. Geochem., Geochemistry Newsletter*, Pap. 27, Spring (1994).
6. Derbyshire, F.J., Davis, A., Lin, R., Stansberry, P.G., and Terrer, M.-T., *Fuel Proc. Technol.*, 12, 127 (1986).
7. Lin, R., Davis, A., Bensley, D.F. and Derbyshire, F.J., *Org. Geochem.*, 11, 393 (1987).

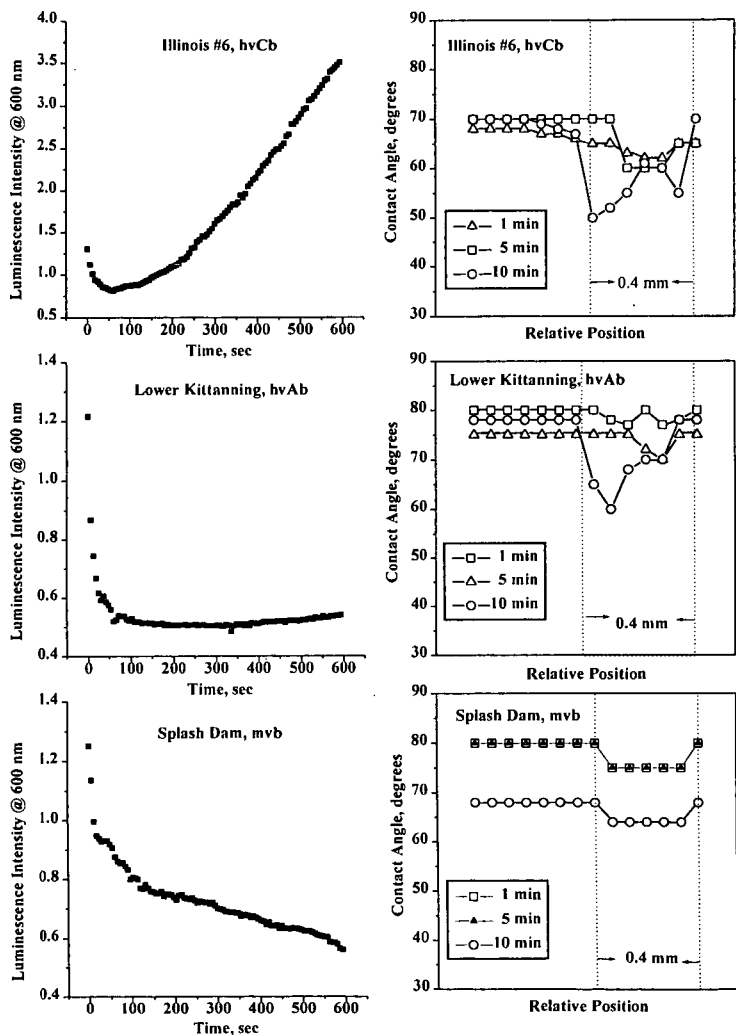


Figure 1. Comparison of luminescence alteration and contact angle measurements on fresh and photooxidized areas of three bituminous coals

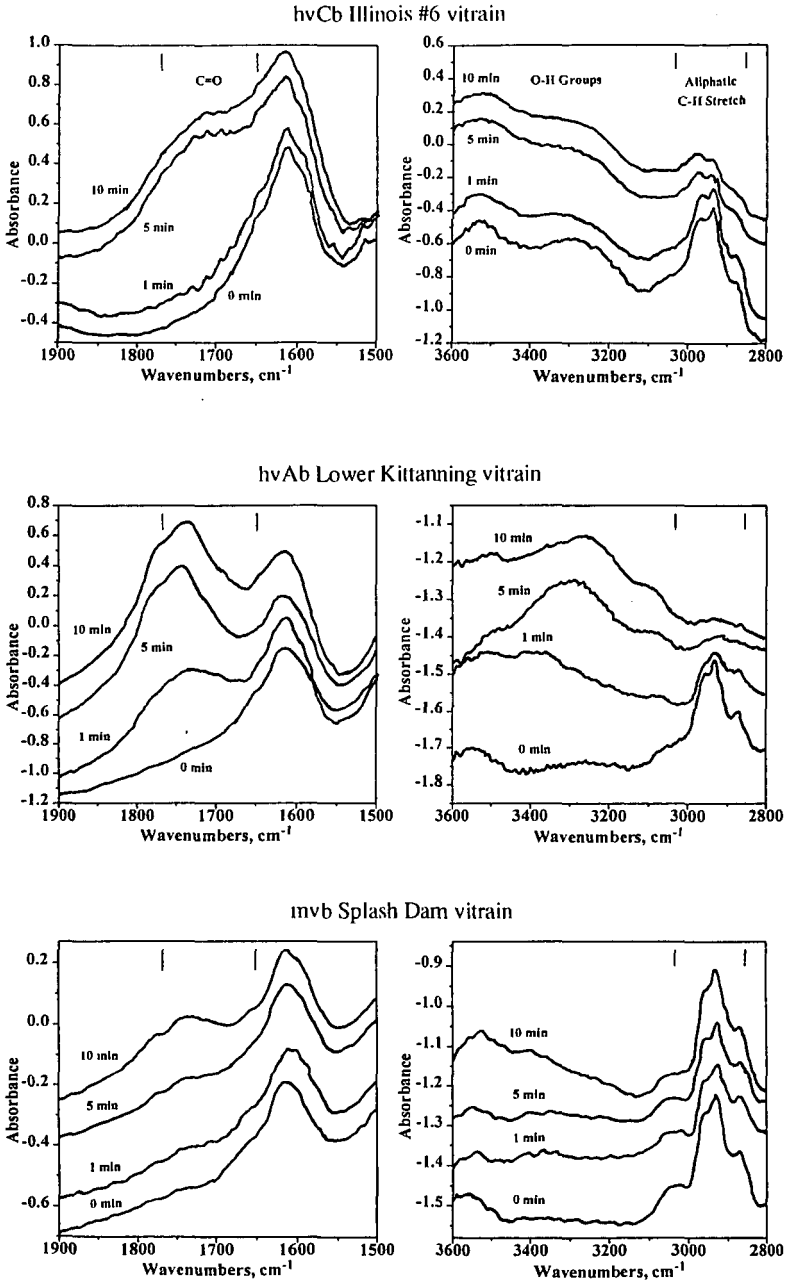


Figure 2. Comparison of FTIR spectral regions for fresh (0 min.) and irradiated surfaces (1, 5 and 10 min.) of three bituminous coals.

## CARBON AS AN OXIDATION CATALYST

D.D. Whitchurst\*  
Mobil Research and Development Corp.  
Central Research Division  
Princeton, NJ 08540

\* Present address - Institute of Advanced Material Study, Kyushu University, Kasuga, Fukuoka 816, Japan

**KEYWORDS** Oxidative dehydrogenation, Carbon catalyst, Mechanism, Surface chemistry

### INTRODUCTION

There are numerous reports in the literature that carbonized metal oxides [1-7], carbons [8] and quinone containing polymers [9,10] can function as oxidative dehydrogenation catalysts. These reports, in combination with earlier work by Roth et al. [11], which showed that carbons can catalyze paraffin dehydrogenation, prompted our interest in assessing the utility of carbons or carbonized metal oxides as light paraffin upgrading catalysts.

It appeared as though there may be a common mechanism or surface chemistry operating in that reported work, so we conducted an extensive review of the literature to help our understanding of the fundamental processes before initiating our work. The purpose of that review was to gain some understanding of the stability and nature of surface functional groups formed on oxidation of carbon surfaces under conditions commonly used in the oxidative dehydrogenation of hydrocarbons in order to interpret mechanisms and potential improvements in oxidative dehydrogenations over carbonaceous catalysts. Several very good reviews on the surface chemistry of carbon do exist, but these do not attempt to interrelate surface chemistry to oxidation catalysis [12-15]. These reviews were utilized extensively in the formulation of our conclusions.

The information which we found relevant to oxidation catalysis from the diverse sources of information on carbon surface chemistry is illustrated in Figure 1. This may be summarized as follows. Carbons heated in inert atmospheres to above 1000-1200°C contain only carbon at their surfaces. All hydrogen and oxygen containing functional groups decompose (degas) below these temperatures to yield water and volatile carbon oxides respectively [12-18]. In degassed graphite, the edges of the basal planes must be composed of carbon in which all of the potential valance orbitals are not satisfied. This chemistry is believed to extend to high surface area carbons as well where the structures are much less developed and the size of the graphitic sheets is very small. One basic question is, just what is the nature of this pure carbon surface? It is known that degassed carbons contain high concentrations of unpaired electrons on their surfaces (as much as 0.2 meq/gm) [14]. In addition, Donnet has proposed that aroxylic radicals may account for many of the free radicals observed on carbons which contain some chemisorbed oxygen [14]. Certainly the surface is rich in free radicals, but what is their geometric configuration and what chemistry do they exhibit?

Two geometric orientations of the edges are possible and these have been referred to as zigzag and armchair. The preference for a given configuration has been shown to be influenced by the atmosphere used in preparation of the surface. Dry conditions favor the armchair configuration and wet conditions favor the zigzag configuration. It is also believed that only these edges interact with oxygen. Apparently, oxygen does not penetrate and react within the lamellar structure [19].

Three possible electronic structures have been proposed [20,21] for the edge carbons in which all of the valance orbitals are not satisfied. These structures contain either (1) one unpaired electron (e.g. free radical), (2) paired electrons (e.g. divalent carbon or carbene), (3) adjacent unpaired electrons or triple bond character (e.g. benzynes).

All of these structures would be expected to interact with oxygen to produce chemisorbed oxygen. The electrical properties of the carbon change drastically as oxygen is chemisorbed. The thermoelectric power of graphite has been shown to be increased algebraically with oxygen concentration on the surface [16a].

Depending on the nature of the carbon structure and the conditions of reaction, one would expect to favor the production of different types of carbon-oxygen functionalities. Freshly degassed carbons begin to chemisorb oxygen at -40°C. Clean carbon surfaces, on contact with oxygen at as low as 200°C evolve volatile carbon oxides simultaneously with the formation of chemisorbed oxygen [17]. At this temperature carbon dioxide is the only gas evolved and about 1 molecule of carbon dioxide is evolved for each three oxygens chemisorbed on the surface [16b]. As the temperature of oxidation is increased, both the rate of chemisorption and volatile carbon oxide evolution increase. The maximum rate of chemisorption occurs at about 400°C [16]. Above 500°C, decomposition of chemisorbed oxygen species becomes significant [16b] and at about 650°C one molecule of CO<sub>2</sub> is evolved for each oxygen chemisorbed. Above 950°C chemisorbed oxygen species are not stable and very little steady state chemisorbed oxygen exists on the surface [16b]. Chemisorbed hydrogen is somewhat more stable and is not completely removed until about 1100°C [16c].

Walker has proposed that there exist two different kinds of reactive surface carbon species [16c]. Both species produce carbon monoxide on reaction with carbon dioxide at gasification temperatures (900-1100°C). One type produces more stable chemisorbed oxygen species C<O>1. The other is much more reactive and produces a less stable chemisorbed oxygen species C<O>2 which decomposes rapidly to gaseous CO and regenerates the free carbon surface. In a parallel reaction C<O>2 also converts to C<O>1 which decomposes much more slowly. The overall rate of gasification thus goes through a maximum and declines to a steady state rate as C<O>1 builds up on the surface. Hydrogen sources, such as H<sub>2</sub> or water inhibit the rate of gasification due to build-up of >CH<sub>2</sub> species which are more stable than carbon oxide surface species. Walker also showed that 2 hydrogens are adsorbed for each site that adsorbs 1 oxygen and he proposed that these sites were carbonyl like [22].

The chemical nature of chemisorbed oxygen has been studied extensively and several excellent reviews are available. Almost every conceivable oxygenated organic functional group has been proposed and detected on

carbon surfaces. Characterization has been done using infra-red spectroscopy, polarography and a variety of diagnostic wet chemical reactions [12,13,14,23].

Methods are well established for the quantitative estimation of acidic groups using selective titrations with bases of varying strength. However, there are some arguments about subtleties in distinguishing between carboxylic acid groups on adjacent vs isolated carbons [12,14]. Quantitative estimation of the content of other functionalities are less reliable and in most types of carbons only about 75% of the oxygen has been accounted for [12,24].

The nature of the functional groups on the surface is very important to the adsorption properties of the carbon and much effort has been devoted to relating functionality to selectivity for gas adsorption [12,15]. It has also been shown that catalyst preparation by impregnation with metal salts is very sensitive to the nature of the functional groups on the carbon surface [23].

The distribution of oxygen containing functional groups on carbon surfaces is dependent on the reagents used to produce the functional groups and the conditions under which the carbon is treated [12,13,14,23]. As our work deals with functionality relevant to oxidative dehydrogenation little discussion will be given on chemical oxidants at low temperatures, other than to say that treatments with strong oxidants, such as HNO<sub>3</sub> lead to very high concentrations of carboxylic acid groups on the surfaces [23]. As will be discussed later, such carboxylic functional groups decompose at the temperatures commonly used in oxidative dehydrogenation.

For a large number of commercial carbons, Studebaker has shown that the relative concentrations of carboxyl, phenol and carbonyl groups are about 3/1/1 respectively. Carbonyl groups represented about 18% of the total chemisorbed oxygen. However only 75% of all of the chemisorbed oxygen was accounted for [24a].

Donnet has shown that gasification of carbons with steam at 900°C yields distributions of carbonyl, lactone and hydroxyl groups that is constant and independent of the degree of gasification of the carbon. This indicates a definite mechanism and stoichiometry for steam gasification [14].

In relating oxygen functionality to oxidative dehydrogenation chemistry, one must consider the conditions under which the reaction is conducted, the rate of oxygen chemisorption, the co-production of volatile carbon oxides, the thermal and oxidative stability of different functional groups and the reactivity of the functional groups with hydrocarbons. Complicating reactions include direct reaction of hydrocarbons with free carbon surfaces, the formation of stable C-H species on the surface and the subsequent oxidation of C-H species on the carbon surface.

Much is known of the thermal stability of different surface functional groups. Table 1 summarizes the temperature ranges of thermal decomposition for the different functional groups and the corresponding gases evolved on decomposition [12-18]. We have previously shown that aromatic ketones and quinones stoichiometrically abstract hydrogen from alkylaromatics, such as tetralin, at 400°C [25]. Thus, one might expect that carbons which form such groups easily and retain them on their surfaces under oxidative dehydrogenation conditions would be good catalysts or potential oxygen carriers. It is interesting to note that the groups which would not be expected to stoichiometrically dehydrogenate hydrocarbons are either quite unstable (decomposing below 500°C) or very stable (decomposing above 700°C).

Putting together the known chemistry of carbon surfaces, reactivity of different organic oxygen functionalities and the observations on oxidative dehydrogenation catalyzed by carbonaceous surfaces, it is possible to propose a catalytic sequence of surface reactions which can explain how carbons can catalyze the oxidative dehydrogenation of hydrocarbons. This proposed mechanism is illustrated in Figure 2.

The desired sequence of surface reactions would be as follows.

- (A) Formation of a reactive free carbon surface, <C><sub>s</sub>
- (B1) Oxidation of the surface to produce an active carbonyl species, <C=O><sub>s</sub>
- (C) Stoichiometric dehydrogenation of the reactive hydrocarbon, forming surface hydrides, <CH<sub>2</sub>><sub>s</sub>
- (D1) Regeneration of the catalyst by oxidation of surface hydrides

This step can also proceed directly to a free carbon surface or surface carbonyl species (A or B).

Side reactions which lead to low selectivity are as follows.

- (E) Excessive Coke Deposition
- (F) Over Oxidation of Surface Carbonyl Species
- (G) Thermal Decomposition of Surface Carbonyl Species
- (H) Over Combustion of Carbon-Overlayers to Pure Metal Oxides
- (B2) Direct Oxidation of Free Carbon Surface to CO and CO<sub>2</sub>

Thus there are a number of competitive surface reactions which dictate catalyst selectivity.

- o Formation of the desired carbon-overlayer is required (A), yet over condensation of hydrocarbons with free carbon surfaces (E) leads to excessive coke formation and eventual loss of catalyst surface area.
- o Formation of the desired surface carbonyl species (B1) is competitive with over condensation (E), carbon-overlayer combustion (B2) and over-oxidation of the carbonyl species (F).
- o Oxidative dehydrogenation to produce the desired product (C) is competitive with surface carbonyl species thermal decomposition (G) and over oxidation of the surface carbonyl species (F).
- o Catalyst regeneration to remove surface hydride species (D1) may be excessive and can remove the carbon-overlayer (D2 or B2).

In the sequence A  $\xrightarrow{\text{R-CH}_2}$  B  $\xrightarrow{\text{O}_2}$  C, a parallel reaction A  $\xrightarrow{\text{R-CH}_2}$  E can occur which leads to product loss by excessive coke formation and perhaps coke which is too labile toward combustion. Thus, catalysts which promote non-selective condensation may exhibit poor selectivity by promoting coke formation. Literature reports on metal oxide catalysts do indicate that excessive acidity of catalysts lead to poor selectivities because of excessive coke build-up and product cracking [6c].

In the sequence  $B \xrightarrow{\text{oxidation}} C$ , a parallel reaction  $B \xrightarrow{\text{oxidation}} G$  (reaction G) can occur which leads to non-productive loss of surface carbonyl species and poor selectivity due to the eventual formation of  $\text{CO}_2$ . As was discussed earlier, surface species such as carboxyl, lactone and lactol are less thermally stable than carbonyls and would be expected to thermally decompose much more readily than the desired surface carbonyl species. Unfortunately, another parallel side reaction,  $B \rightarrow C \rightarrow F$  (thermal decomposition of  $\text{<O>s}$ ) also can occur which would lead to non-productive loss of surface carbonyl species. Thus, high hydrocarbon partial pressures should enhance reaction C over competitive reactions G and F. Alternatively, high hydrocarbon partial pressures would appear to inhibit reactions G and F.

If the above proposed mechanism is correct, one should be able to produce, isolate and identify oxidized carbon surfaces which will stoichiometrically react with hydrocarbons to produce olefinic products in the temperature range of 400-500°C. To test this postulate, we obtained a series of different carbons, oxidized them under a variety of conditions, determined their thermal stability and reacted them with selective reagents to determine the reactive oxygen content of their surfaces. The results of those studies is the subject of this paper.

## EXPERIMENTAL

The carbons used in this study were obtained from the following sources.

Amoco AX-21 - Dr. K.K. Robenson of Amoco Corporation.  
Anderson AX-21 - Anderson Development Company, Adrian, Michigan  
Barneby-Sutcliff 207-C & 209-C - Barneby-Sutcliff Corp., Columbus Ohio.  
Darco activated carbon - American Norit Co. Inc.  
Animal Bone Charcoal - EM Sciences - Macalaster-Bicknell Co.  
Wood Charcoal - Matheson Colman & Bell Manufacturing Chemists  
PVDC Carbon - Dr. D.F. Quinn of the Royal Military College, Kingston, Ontario.  
Si/C carbon, whisker by-product - Dr. D. J. Rhodes of Advanced Composite Materials Corp.  
C60 Soot - MER Corporation.  
Graphite flake - Aldrich Chemical Co. Inc.

Thermogravimetric analyses were obtained on a DuPont Series 99 Thermal Analyzer, using ultra pure purge gases. Each analysis consisted of a sequence of three programmed heatings and is referred to as STPD.

- 1) Argon Purge 20°C/min 25 to 750°C Cool to 25°C
- 2) Air Purge 20°C/min 25 to 450°C Cool to 25°C
- 3) Argon Purge 20°C/min 25 to 750°C Cool to 25°C

The % active oxygen ( $\text{<O>s}$ ) was estimated from the weight loss between 550 and 750°C in step 3.

The procedure for estimating the % active oxygen ( $\text{<O>s}$ ), by chemical reaction, consisted of preoxidizing the material to be studied in air in a muffle furnace at 450°C for 15-60 min to provide about 30% burnoff of the carbon. The sample (0.2 to 0.4g) was then weighed into a 10cc tubing bomb and 1.4g of a reagent consisting of 48wt% tetralin, 4wt% 1-methylnaphthalene and 48wt% diphenylether was added. The tube contents were purged with  $\text{N}_2$  then sealed. The tube was placed in a muffle furnace, set at 450°C, for the desired reaction time then removed from the furnace and quenched in a water bath. A sample of the liquid product was taken and analyzed by gas chromatography.

Oxidative dehydrogenation reactions were conducted at atmospheric pressure in a quartz down flow reactor. Reactions were carried out by feeding EB to the preheated quartz reactor bed, which was then blended with a mixture of 5%  $\text{N}_2/95\% \text{O}_2$ . Liquid samples were collected in a chilled trap (2°C), while gas samples were collected in collection tubes. Good liquid mass balances could be obtained at times on stream of greater than 20 min. Liquid analyses were aided by dilution of the liquid products with acetone containing 10.0% 3-hexanone as an external standard, this solvent also provided a means to overcome niscibility problems associated with water.

## RESULTS AND DISCUSSION

**Thermal stability of oxidized carbon surfaces** - In the carbon community, a standard procedure has evolved for the characterization of carbons by programmed thermal decomposition is and referred to as TPD [16] and references therein. This procedure consists of linear programmed thermal decomposition (3°C/min) of the carbon being studied in nitrogen atmosphere from 300 to 1300°C coupled with simultaneous detection of  $\text{CO}$ ,  $\text{CO}_2$  and often water and hydrogen. Typically,  $\text{CO}_2$  is predominantly evolved below 550°C. For almost all carbons the maximum rate of evolution of  $\text{CO}_2$  occurs at 500°C and  $\text{CO}$  at 600°C [12]. Coltharp has shown that for a wide variety of carbons, the pattern of  $\text{CO}_2$  evolution varies considerably, perhaps due to different conditions in which the carbons were oxidized. However, the patterns of evolution of  $\text{CO}$  were quite similar for diverse carbons [18].

Unfortunately, this procedure only provides the total amount and distribution of gases from the carbon surface. In its present form, it cannot be used to estimate the concentration of reactive chemisorbed oxygen that is needed for oxidative dehydrogenation catalysis. As discussed above, carbonyl groups (ketones and quinones) are the most likely oxygen containing species which can promote oxidative dehydrogenation of hydrocarbons. Therefore if one could estimate the concentration of such carbonyl species on carbon surfaces, it may be possible to predict the dehydrogenation activity of carbons. The content of carbonyl groups on carbon surfaces have been estimated to be about 18% of the total chemisorbed oxygen [12a].

From the known thermal behavior of different chemical functionalities on carbons, it may be possible to estimate the concentration of carbonyls by determining the weight loss or amount of carbon monoxide evolved from a given carbon in a specific temperature range. As shown in Table 1, carbonyl groups have reasonable thermal stabilities below 550 °C but decompose in the range of 550-750°C. Functional groups which decompose at low temperatures (<550°C) or at very high temperatures (>750°C) are not expected to be important in oxidative dehydrogenation catalysis. On this assumption, we conducted a series of thermal analyses on a variety of carbons to see if major differences could be observed in a systematic way.

The carbons we used are described in the experimental section. Their physical properties varied widely in terms of surface area, degree of carbonization and ash content. To evaluate their thermal behavior each carbon was pretreated at 750°C in oxygen free argon to clean its surface. Each carbon was then oxidized in diluted air (14.7% O<sub>2</sub>) by programming to 450°C and cooling to room temperature in that atmosphere. The thermal decomposition profile of the oxidized carbon was then determined by programmed decomposition up to 750-800°C in oxygen free argon. The sequential programmed thermal decomposition analysis will be referred to as SPTD.

Table 2 summarizes the observed rates of weight loss in each cycle at 400°C and the estimated amounts of chemisorbed oxygen found as either CO<sub>2</sub> or CO assuming that weight loss below 550°C was primarily CO<sub>2</sub> and between 550 and 750°C oxidatively active carbonyls decomposed to evolve primarily CO, as discussed above.

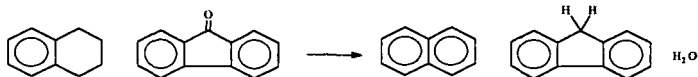
With the exceptions of animal bone charcoal and C60 soot the data appear to fall within the range of oxygen contents reported in the literature [12a]. The animal bone charcoal results may have been exaggerated due to the high correction factors necessary for this high ash content material. In the case of C60 soot it is believed that high contents of low molecular weight species vaporized from the sample simultaneously with the carbon oxide decompositions. The initial Argon cycle resulted in the loss of a great deal of weight in the temperature range in which a pure sample of C60 also rapidly volatilized. This result is interesting in that the C60 soot is believed to contain high concentrations of tubular fullerenes. This oxidation-thermal decomposition cycle may offer a route to the production of higher yields of lower molecular weight fullerenes from C60 soots.

In comparing the rates of weight loss in each cycle of the SPTD analyses 400°C, where the maximum rate of oxygen chemisorption has been reported [12a], it is interesting to note that only C60 soot showed a positive weight change at this temperature. There appeared to be two sets of sample behavior. Those with high ash (particularly alkaline ash) and those with low ash. For low ash samples, the surface area of the parent carbon offered the best correlation with the rate of weight loss. In the case of high ash samples, the rates of weight loss correlated well with ash content. However, two high ash samples had low rates of oxidation, silicon carbide by-product and coal derived charcoal (Darco). The majority of the ash constituents of the silicon carbide by-product was in fact SiC and would be expected to be inert. Coal charcoal ash is primarily silica-alumina and would not be expected to catalyze carbon oxidation. The other carbons ashes were found to be alkaline and would therefore be expected to catalyze such oxidations. Animal bone charcoal was not found to be highly alkaline but is composed primarily of calcium phosphate (hydroxyapatite) [26]. Calcium is known to be an active catalyst for carbon oxidation [16d].

On comparing the rates of thermal decomposition of oxidized carbons with the rates of oxidation in Table 2, it appears that carbons which oxidize rapidly also decompose rapidly. At this time it is not clear if ash components catalyze the thermal decomposition or they change the selectivity in the formation of different functional groups on the carbon surface during the oxidation cycle.

The results of these studies indicate that oxidized carbon surfaces can accommodate 1 to 10% by weight oxygen in the form of carbonyl functional groups. Such groups should have potential as stoichiometric oxidation reagents. In all cases the formation of these active groups occurs simultaneously with the oxidation of a portion of the carbon to volatile oxides. Thus, the selectivity for oxygen utilization in the formation of these groups will always be limited. This selectivity appears to be lower for carbons containing alkali or alkaline earth impurities. Thus supported carbons may require careful preparation. However, it may be possible to use carbons as oxygen carriers in which active oxygen species are formed in air then utilized as oxidation reagents in contact with hydrocarbons.

**Measurement of the active oxygen capacity of carbons by stoichiometric reactions.** Unfortunately, the STPD results does not give a quantitative measure of the reactive oxygen content of carbons. In past work involving hydrogen donor chemistry, we have described how it is possible to quantitatively measure either hydrogen abstraction capacity of a solid or hydrogen donor capacity of a liquid by a test chemical reaction. We showed that aromatic ketones and quinones stoichiometrically abstract hydrogen from alkylaromatics, such as tetralin, at 400°C [25]. Thus, one might expect that carbons which form such groups easily and retain them on their surfaces under dehydrogenation conditions would be good catalysts or potential oxygen carriers. We endeavored to use this same technique at 450°C to assess the potential of various carbons as dehydrogenation reagents and the results are presented in this section. The test reaction may be illustrated simply with model compounds as follows.



The results of model compound scoping experiments are presented in Table 3. It can be seen that the results are quite quantitative. However, the chemistry of quinones was not found to agree with proposals in the literature that quinones would convert to hydroquinones. Instead, we found that only one of the carbonyls of phenanthrene type quinones were active, as after hydrogen abstraction by the first carbonyl, the intermediate monocarbonyl rearranged to a stable monophenol which did not react further. Anthracene type quinones behaved like two independent carbonyls and did not form hydroquinones. Instead, they converted to dihydroanthracene. This compound was metastable under the reaction conditions and underwent some disproportionation.

In addition to stoichiometric hydrogen abstraction it was anticipated that some catalysis of hydrogen transfer or equilibrium dehydrogenation might occur. Roth reported that carbons supported on alumina were extraordinary catalysts which in some cases rivaled the performance of commercial supported noble metal catalysts [11]. Indeed, when oxidized carbons were tested with the test reagent, catalysis was observed. Thus, when attempting to relate the amount of naphthalene formed from tetralin in these tests, it was necessary to subtract out catalytic contributions of the carbons. This correction was possible by the inclusion of 1-methylnaphthalene in the reagent mixture which measured the kinetically parallel reactions of catalytic tetralin dehydrogenation and catalytic hydrogen transfer between tetralin and 1-methylnaphthalene. In addition corrections also had to be made for thermal isomerization of tetralin to 1-methylindan, the thermal dehydrogenation of tetralin and a small amount of hydrogenolysis of the diphenylether co-solvent.

Two methods of estimation were used. For low conversions of tetralin, direct stoichiometric calculations were employed. For high conversions of tetralin, the equilibrium distribution of tetralin/naphthalene/H<sub>2</sub> was calculated assuming that hydrogen lost in the formation of water was an indicator of the active oxygen content of the carbons.

Surprisingly, some carbons were almost as catalytically active as 5%Pd/charcoal for hydrogen transfer and dehydrogenation. A general observation was that highly graphitic carbons exhibited high catalytic activities and non-graphitic carbons exhibited high activities for stoichiometric reactions of active oxygen. Several carbons, when oxidized, were found to contain as much as 10wt% active oxygen. Petroleum cokes could also be oxidized to produce materials with as much as 5wt% active oxygen. Carbonized CaPO<sub>3</sub> catalysts produced during oxidative dehydrogenation studies were found to contain active oxygen contents (carbon only basis) that were comparable to some of the most active, highest capacity pure carbons examined. The results are summarized in Table 4.

#### CONCLUSIONS

The results of these studies indicate that oxidized carbon surfaces can accommodate 1 to 10% by weight oxygen in the form of carbonyl functional groups which are potential stoichiometric oxidation reagents. In all cases the formation of these active groups occurs simultaneously with the oxidation of a portion of the carbon to volatile oxides. Thus, the selectivity for oxygen utilization in the formation of these groups will always be limited. This selectivity appears to be lower for carbons containing alkali or alkaline earth impurities. Thus, supported carbons may require careful preparation. However, it may be possible to use carbons as oxygen carriers in which active oxygen species are produced in air and then utilized as oxidation reagents in contact with hydrocarbons. The mechanism of oxidative dehydrogenation over carbonaceous catalysts appears to be consistent with this chemistry.

#### REFERENCES

1. T.G. Alkhazov, A.E. Lisovskii, M.G. Safarov and A.M. Dadasheva, *Kinet. Katal.* 13, 509 (1972).
2. P. Ciambelli, S. Crescitelli, V. DeSimone and G. Rosso, *Chim. Ind. Milan* 55, 634 (1973).
3. K. Tazaki, R. Kitahama, F. Nomura and T. Yokoji, *Japan Pat.* 74-39246; *Chem. Abst.* 83, 44002v (1975).
4. R. Fiedorow, W. Przystajko, M. Sopa & I.G. Dalla-Lana, *J. Cat.* 68, 33 (1981)
- 5a. G. Emig & H. Hofmann, *J. Cat.* 84, 15 (1983).
- 5b. A. Schraut, G. Emig & H.-G. Sockel, *Appl. Cat.* 29, 311 (1987).
- 5c. A. Schraut, G. Emig & H. Hofman, *J. Cat.* 112, 221 (1988).
- 6a. G.E. Vrieland, *J. Cat.* 111, 1 (1988).
- 6b. G.E. Vrieland, *J. Cat.* 111, 14 (1988).
- 6c. G.E. Vrieland & P.G. Mennon, *Appl. Cat.* 77, 1 (1991).
7. L.E. Cadus, O.F. Gorzic and J.B. Rivarola, *Ind. Eng. Chem. Res.*, 29, 1143 (1990).
- 8a. G.C. Grunewald & R.S. Drago, *J. Mol. Cat.* 58, 227 (1990).
- 8b. G.C. Grunewald & R.S. Drago, *J. Am. Chem. Soc.* 113, 1636 (1991).
9. J. Manassen & SH. Khalif, *J. Cat.* 13, 290 (1969).
- 10a. Y. Iwasawa, H. Nobe and S. Ogasawara, *J. Cat.* 31, 444 (1973).
- 10b. Y. Iwasawa & S. Ogasawara, *J. Cat.* 37, 148 (1975).
- 11a. J.F. Roth & A.R. Schaefer, *Belgain Patent* 682,863 (1966).
- 11b. J.F. Roth & A.R. Schaefer, *U.S. Patent* 3,356,757 (1966).
- 11c. J.F. Roth, J.B. Abell & A.R. Schaefer, *I&E Prod. R&D*, 7, 254 (1968).
- 11d. J.F. Roth, J.B. Abell, L.W. Fannin & A.R. Schaefer, *ACS Petr. Div. Prep. New York*, Sept. 1969, p.D146.
- 11e. J.F. Roth, J.B. Abell, L.W. Fannin & A.R. Schaefer, *Adv. Chem.* 97 193 (1970).
- 12a. B.R. Puri, *Chem. & Phys. of Carbon*, 6, 191 (1970).
- 12b. B.R. Puri, G.K. Sharma & S.K. Sharma, *Proc. 5th Conf. on Carbon*, 65 (1962)
- 12c. B.R. Puri, G.K. Sharma & S.K. Sharma, *J. Indian Chem. Soc.* 44, 64 (1967).
- 13a. H.-P. Boehm, *Angew. Chem.*, 5, 533 (1966).
- 13b. H.-P. Boehm, *Adv. Cat.* 16, 179 (1966).
14. J.B. Donnet, *Carbon*, 6, 161 (1968).
15. J.S. Mattson & H.B. Mark Jr., *Activated Carbon*, Marcel Dekker Inc., New York, Chapt. 3 (1971)
- 16a. P.L. Walker Jr., L.G. Austin & J.J. Tietjen, *Chem. & Phys. Carbon*, 1, 327 (1965).
- 16b. F.J. Vastola & P.L. Walker Jr., *J. Chim. Phys.* 58, 20 (1961).
- 16c. M. Shelef & P.L. Walker Jr., *Carbon*, 5, 93 (1967).
- 16d. P.L. Walker Jr., M. Shelef, & R.A. Anderson, *Chem. & Phys. of Carbon*, 4 287 (1968).
- 16e. G. Tremblay, F.J. Vastola & P.L. Walker Jr., *Carbon*, 16, 35 (1978).
17. W. V. Lobenstein & V.R. Deitz, *J. Phys. Chem.*, 59, 481 (1955).
18. M.T. Coltharp & N. Hacherman, *J. Phys. Chem.*, 72, 1171 (1968).
- 19a. G.R. Henning, *Proc. 5th Conf. on Carbon*, 1, 143 (1962).
- 19b. G.R. Henning, *Z. Elektrochem.*, 66, 629 (1962).
20. C.A. Coulson, *Proc. 4th Conf. on Carbon*, Pergamon Press (1962) p.215.
21. F.J. Salzano, *Carbon*, 2, 73 (1964).
22. J.F. Strange, Ph.D. Thesis, Penn. State U. (1964).
- 23a. F. Rodriguez-Reinozo and A. Linares-Solano, *Chem. & Phys. of Carbon*, 21, 1 (1988).
- 23b. C. Prado-Burguete, A. Linares-Solano, F. Rodriguez-Reinozo & C. Salinas-Martinez De Lecea, *J. Cat.* 115, 98 (1989).
- 23c. F. Rodriguez-Reinozo, M. Molina-Sabio & M.A. Munecas, *J. Phys. Chem.* 96, 2707 (1992).
- 23d. M. Molina-Sabio, M.A. Munecas-Vidal & F. Rodriguez-Reinozo, "Characterization of Porous Solids", Elsevier Science, Amsterdam (1991), p. 329.
- 24a. M.L. Studebaker, E.W.D. Huffman, A.C. Wolfe & L.G. Nabors, *I & E Chem.* 48 162 (1956)
- 24b. M.L. Studebaker, *Rubber Age (N.Y.)*, 80, 661 (1957).
- 25a. D.D. Whitehurst, M. Farcasiu, T.O. Mitchell & J.J. Dickert Jr., "The Nature and Origin of Asphaltene in Processed Coals", EPRI- AF-480, July 1977, Chapt. 8.
- 25b. D.D. Whitehurst, M. Farcasiu & T.O. Mitchell, "Coal Liquefaction- The Chemistry and Technology of Thermal Processes", Academic Press, New York (1980), Chapt. 8.
26. *Encyclopedia Britanica* William Benton, Publ., Vol.B (1964) p.906.

**TABLE 1**  
**THERMAL DECOMPOSITION OF ORGANIC OXYGEN COMPOUNDS**

Functional Group	Decomposition Temp. Range (°C)	Gas Evolved
Carboxylic acid	200-600	CO <sub>2</sub>
Aldehyde	<400	CO
Lactone/Lactol	200-600	CO <sub>2</sub> & CO
Ketone/Quinone	600-1000	CO
Phenol	600-1000	CO
Aromatic Ether	>700	CO
Anhydride	>700	CO <sub>2</sub> & CO

**TABLE 2**  
**ESTIMATED REACTIVITIES AND OXYGEN CONTENTS OF CARBONS VIA STPD**  
(Ash free carbon basis)

Carbon	Rates of Weight Loss at 400°C (wt%/min)					Calculated % Chemisorbed O		
	Initial	After air	Argon-1			From CO <sub>2</sub>	From CO	Total
			Argon-1	Air	Argon-2			
C60 Soot	0	93	-4.78	0.72	-0.51	0.38	21.89	22.26
Animal Bone Charcoal	86	12	-5.24	-50.1	-15.7	22.47	15.38	37.85
Wood Charcoal	13	49	-4.82	-16.6	-2.37	3.31	8.40	11.71
PVDC Carbon	0	21	-0.72	-0.72	-0.37	1.61	4.61	6.22
Amoco AX-21	2	25	-1.51	-4.45	-0.24	2.57	2.55	5.12
Darco (20-40 mesh)	12	10	-0.84	-0.12	-0.56	1.15	1.70	2.84
Si/C By-product	34	8	-0.36	-1.36	-0.05	1.30	1.57	2.87
Barneby-Sutcliff 207C	3	15	-0.97	-6.29	-0.47	0.87	1.28	2.15
Graphite	0	2	-0.19	-0.07	-0.02	0.12	0.32	0.43

**TABLE 3**  
**Stoichiometry and Rate Constants for Reactions of Model Compounds With the Test Reagent**

Compound	Mol. Wt.	Wt% O	Rx Time (min)	% Conv	Hydrogen Consumption		Reaction Rate Constants (1000xmmol prod/g.rgt/g.matrl/min)		
					Theory	Observed	k <sub>mind</sub>	k <sub>resh</sub>	k <sub>met</sub>
Benzophenone	182	8.8	30	7.2	4	4.3	21	21	0
Benzophenone	182	8.8	60	27.8	4	4.1	33	21	0
Fluorenone	180	8.9	60	16.4	4	4.9	21	54	0
9-Anthrone	194	8.2	60	97	4.4	4.7	28	100	1
Antraquinone	208	15.4	30	97	6.6	6	24	364	1
Phenanthrenequinone	208	15.4	30	100	4.2	4.2	10	255	1
Bi2O3 (42%)*	466	10.3	60	6	4.6	6	31	41	0
V2O5 (52%)*	182	17.6	60	4	3.9	3.9	20	94	2

\* Metal oxides were supported on inert carriers, values shown are for pure metal oxides

TABLE 4

COMPARISONS OF THE ESTIMATED VALUES FOR ACTIVE OXYGEN CONTENTS OF CARBONS  
(Weight % <O>s , ash corrected values)

Material	Rx Time (min)	% Carbon	Estimated wt% <O>s		
			Stoich.	Equil.	SPTD
PVDC	60	100	4.8	4.6	
AX-21 (41)	240	97	25.6	28.8	2.6
AX-21 (41)	60	97	7.1	7.0	2.6
AX-21 (41)	60	97	6.9		2.6
AX-21 (41)	30	97	2.0		2.6
Used AX-21 (41)	60	97	3.2		
AX-21 (93)	60	71	16.7		
Barney-Sutcliff 207c	240	95	8.2	6.0	1.3
Barney-Sutcliff 207c	60	95	3.9	1.7	1.3
Barney-Sutcliff 207c (dry)	30	95	2.8	1.3	
Barney-Sutcliff 207c (wet)	30	95	2.2	1.3	
Barney-Sutcliff 209c	60	95	1.0		
Darco (20-40 mesh)	60	82	6.1	5.2	1.7
Darco (20-40 mesh)	60	82	2.6	1.7	
Norit Activated Carbon	60	84	2.2		
Wood Charcoal	60	78	6.6	8.4	
Animal Bone Char	60	2	44.8	15.4	
Petroleum Shot Coke	60	100	5.3		
Petroleum Sponge Coke #1	60	100	4.1		
Petroleum Sponge Coke (as rec)	60	100	1.1		
			<u>No Cat. Max.</u>		
C60 Soot	60	100	0.3	9.4	21.9
Si/C By-product	60	52	-1.6	2.0	1.6
Graphite	60	100	-1.8	0.2	0.3
Graphite	60	100	-1.7	0.2	0.3
C/CaPOx (Run 228-4)	60	2.2	1.4	13.4	
C/CaPOx (Run 228-5)	60	1	-14.1	14.4	
CaPOx (Starting material)	60	0	-0.2	0.0	

FIGURE 1

CHEMISTRY OF CARBON SURFACES

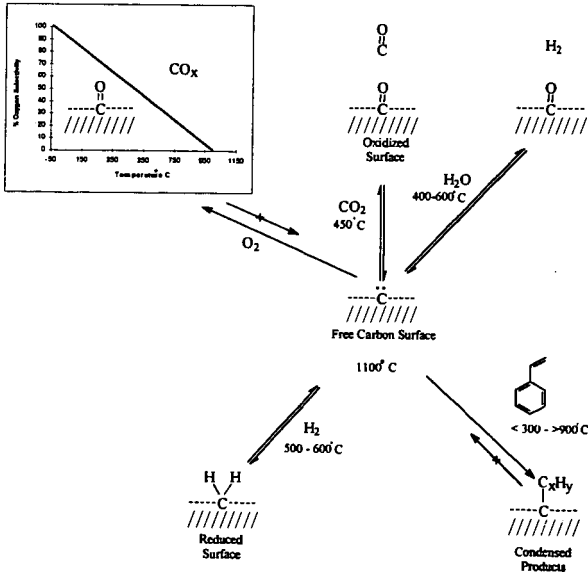


FIGURE 2  
 CATALYTIC SEQUENCE IN OXIDATIVE DEHYDROGENATION

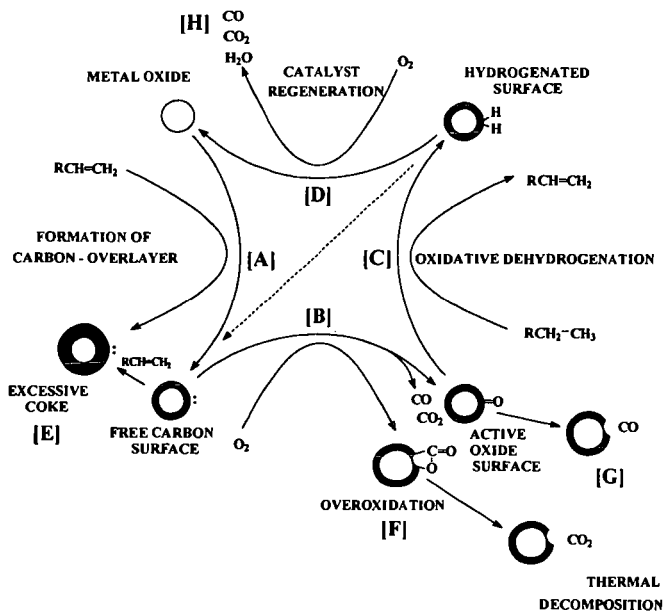
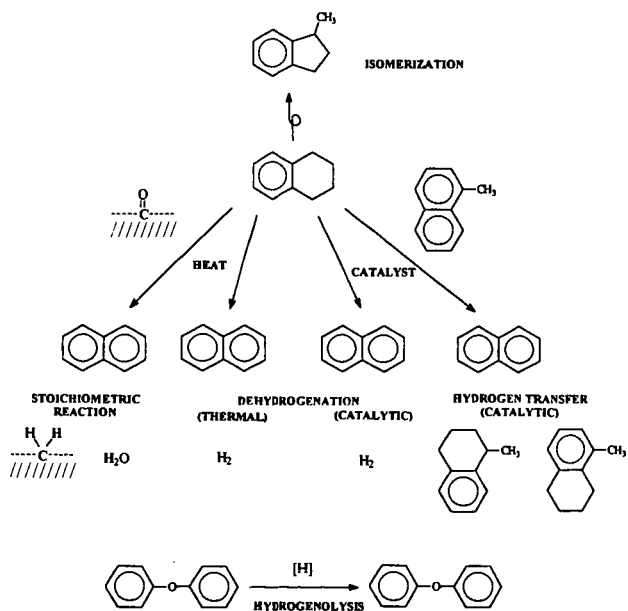


FIGURE 3  
 REACTIONS OF THE TEST REAGENT



# OPTICAL SPECTROSCOPY OF A QUANTUM CARBON WIRE

Peter C. Eklund<sup>1</sup>

Center for Applied Energy Research and  
Department of Physics and Astronomy  
University of Kentucky, Lexington, KY 40506

Keywords: carbon nanotubes, Raman scattering, quantum confinement

**Abstract** Raman Spectroscopy has been used to probe the vibrational modes of carbon nanotubes. The Raman spectrum of this new form of carbon is very different from that observed for graphite (the nanotube's flat parent) and these differences can be understood as a result of the cyclic boundary condition imposed on a graphene sheet rolled up to form a seamless nanotube. Optical resonances are observed which are associated with the one dimensional character of the electronic states of these novel quantum wires.

## INTRODUCTION

Single wall nanotubes (SWNTs) were discovered in 1993 in the carbonaceous by-products from an arc discharge between carbon electrodes in an inert atmosphere [2,3]. They have been observed directly in electron microscopes and in scanning tunneling microscopes. In this paper, we wish to explore the special nature of these one dimensional (1D) carbon quantum wires using Raman spectroscopy. The quantum effects we observe here cannot be observed in the so-called "multiwall carbon nanotubes" (MWNTs) which were discovered a few years earlier also in the soot from a carbon arc[4]. These MWNTs are comprised of a series of concentric SWNTs with an inter-shell spacing of about 3.4 Å. The inner diameter of the MWNT is typically 5-10 times larger than a SWNT. As small as these diameters are in terms of a micron scale, they are too large to observe the quantum size effects we observe in SWNTs with diameters ~ 1nm.

In Fig. 1 the  $sp^2$  based structure of a seamless carbon nanotube is shown schematically. The hexagonal arrangement of C-atoms, identical to that in flat carbon sheets of graphite, are apparent in the figure. Three different subclasses of seamless nanotubes can be formed: armchair ( $n, n$ ), zigzag ( $n, 0$ ) and chiral ( $n, m \neq n$ ) where the integers  $n$  and  $m$  are used to define the symmetry of the nanotube [4]. Understanding how to compute  $(n, m)$  are not important to understanding the principle results discussed here. It is of interest to know only that "armchair" and "zigzag" tubes have rows of hexagons aligned parallel to the tube axis and chiral tubes can be formed such that the hexagon rows spiral up along the tube axis. The tube shown in Fig. 1 is a (9,9) armchair tube. The diameter of an armchair tube is given by  $D(\text{Å}) = 1.357n$ , so that a (10,10) nanotube has a diameter of 13.57 Å.

Until recently, research on the physical properties of these quantum carbon wires have been slowed by the fact that previous arc discharge methods produced mostly carbon soot and only a few % carbon nanotubes[4]. Thus experimental signals in these samples were often dominated by the response of the soot. Recently, a laser ablation technique was discovered at Rice University which produced over 70% tubes [5]. Using microfiltration, we have been able to separate the carbon nanosoot from the tubes and study reasonably pure tube samples by Raman spectroscopy. Details of the laser-assisted process developed at Rice University are available elsewhere [5]. Briefly, a carbon target containing 1-2% Ni/Co catalyst is maintained in flowing Ar in an oven (1200 °C). The carbon target is vaporized by a two-pulse sequence from a YAG and frequency-doubled YAG laser at a 10 Hz repetition rate. Nanotubes (>70%) and carbon nanospheres (~30%) and fullerenes (~1-2 %) form in the hot carbon plasma and drift downstream under flowing Ar where they are collected on a water-cooled cold finger. The carbon material was first soaked in  $CS_2$  to remove solubles (i.e., fullerenes) and the insolubles were then subjected to microfiltration to physically separate the tubes and soot. This was accomplished by dispersing the material in benzalkonium chloride using ultrasound.

The resulting carbon material appears in scanning electron microscopy (SEM) images as a mat of carbon fibers. Transmission electron microscopy (TEM) was used to measure the fiber diameter. Under high resolution it was observed that the tubes were arranged into regular bundles of single-wall carbon nanotubes. These bundles, or crystalline ropes, can be seen directly in the bright field TEM image or indirectly by the electron diffraction pattern which stems from the ordered stacking of carbon cylinders. Looking at the bundle end-on, the individual tubes can be seen to organize into a two-dimensional triangular lattice. The TEM images of, and electron diffraction patterns from these crystalline ropes are shown in Figs. 2a,b. In Fig. 2c we show the size distribution determined from bright field TEM images. The mean tube diameter was also determined by x-ray diffraction (XRD). XRD and TEM yielded slightly different values for the mean tube diameter  $D$  which must stem from a non-statistical distribution of tubes selected for study in the TEM. A mean value for  $D$  consistent with a (10,10) tube was determined by XRD, in

<sup>1</sup> This paper is based, in part, on results to appear in Ref. 1.

agreement with previous XRD data on similar tubes[5]. Our bright field TEM data (Fig. 2c), however, arrived at a slightly smaller mean D value, more consistent with a (9,9) tube. As can be seen from Fig. 2c, the diameter distribution for the tubes is consistent with armchair symmetry tubes (see the tick marks in the figure) associated with the range of n-values 8-11.

In Fig. 3, we display the Raman spectrum (300 K) for purified single wall nanotubes obtained in the backscattering geometry using 514 nm Ar laser radiation. For comparison, the calculated Raman spectrum is shown below for n=8-11 armchair tubes. The frequencies were calculated in a phenomenological force constant model using the same C-C force constants used to fit vibrational data for a flat graphene sheet [6]. Note that sections of the experimental spectrum have been scaled vertically (as indicated) to best expose the rich detail. Furthermore, the frequency scale has been expanded for the highest frequency region. The theoretical Raman intensities were calculated using a bond polarizability model by Subbaswamy and co-workers [7]. The mode assignments are summarized in Table 1 and compared with theory. Further polarized Raman studies will be necessary to confirm the symmetry assignments. It may be noticed that the some of the experimental bands are narrow and some are broad. This difference is attributed to an inhomogeneous line-broadening mechanism based on the theoretical observation that particular vibrational modes exhibit a strong tube diameter dependence, while others exhibit a rather weak dependence. Thus considering that our sample contains a distribution of tube diameters, the Raman lines can be sharp (similar to a linewidth in graphite  $\sim 6 \text{ cm}^{-1}$ ) or much broad, depending on whether or not the mode frequency is strongly diameter-dependent. The intense line seen at  $186 \text{ cm}^{-1}$  in Fig. 3 is identified with the radial breathing mode in which all C-atoms are displaced radially outward in phase and the strong lines observed near  $1600 \text{ cm}^{-1}$  are related to the intralayer vibrations in graphite which are observed at  $1582 \text{ cm}^{-1}$ . In the nanotube, the cyclic boundary conditions around the tube waist activate new Raman and IR modes that are not observable in a well-ordered flat graphene sheet or in graphite--this is the first consequence of the one-dimensional (1D) nature of the nanotube. The second, to be discussed below, is the quantum confinement of the conduction electrons which gives rise to resonant Raman scattering.

The resonant nature of the Raman scattering process is clear from Fig. 4 which shows the dramatic effect on the distribution of line intensity on the frequency (or wavelength) of the excitation laser. The data were all taken at the same temperature on the same sample. Shown in the figure are spectra taken with four different lasers at the (low) power densities indicated. A closer inspection of the figure reveals that not only are the intensities changing dramatically with laser frequency, but so are the Raman line frequencies!! The former effect is typical of resonant Raman scattering in many solid, gas and liquid samples, whereas the latter is a manifestation of a series of resonances each identified with different tube diameters (e.g., (n,n)). In general, resonantly enhanced Raman scattering occurs when the energy of the incident photon matches the transition energy of a strong optical absorption band [8]. Normally, the Raman line intensity can jump by several orders of magnitude, but the Raman line frequency is fixed or varies very slightly. In the present work, large shifts in frequency are also observed which is quite unusual.

We now provide a simple explanation for this observation based on tube-diameter-dependent optical absorptions which stem from the 1D nature of the single wall carbon nanotube. A more complete theoretical explanation will be forthcoming [7]. For large enough tube diameter, the character of the electronic states in a carbon nanotube should be essentially independent of tube diameter (or n in (n,n)) and should resemble closely that of a flat graphene sheet. These larger tubes therefore should respond to the excitation laser as does graphite, or more precisely a single graphene sheet, exhibiting no strong resonance(s) in the region of interest here and only one Raman line at  $\sim 1582 \text{ cm}^{-1}$ . This is what is observed, for example, in much larger diameter multiwall carbon nanotubes. A change in laser excitation wavelength (or frequency) is found to produce small changes in the Raman intensity and extremely small (if detectable) changes in the frequency of the  $1582 \text{ cm}^{-1}$  mode. The large shifts in Raman line frequency we observe are therefore identified with a diameter-dependent optical absorption which promotes resonant scattering from particular diameter tubes. The shifting frequency is both the result of the sample being a collection of different diameter tubes and the fact that these different diameter tubes have different optical resonances. In 1D systems it is well known that  $E^{-1/2}$  singularities exist in the electronic density of states (DOS). These singularities manifest themselves as spikes in the DOS calculated for n=8,11 armchair tubes and shown in Fig. 5; the Fermi energy ( $E_F$ ) is taken as the energy zero. The allowed optical transitions for these tubes can be shown to be between filled states in spikes below  $E_F$  ( $v_1, v_2$ ) to empty states above  $E_F$  ( $c_1, c_2$ ). As required to explain our experimental results, the energy separation between these mirror image spikes must be diameter (n) dependent consistent with the results of Fig. 4. As one can now appreciate, Raman scattering from a (n,n) tube will dominate the spectrum when the laser photon energy matches the energy difference between spikes for that (n,n) DOS. The center of gravity of each Raman band then shifts to the frequency of the (n,n) vibrational mode being resonantly driven by the laser field.

Thus, the unusual laser frequency dependence of the Raman spectra of carbon nanotubes shown in Fig. 4 is a direct consequence of 1D quantum confinement effects in carbon nanotubes. Further work is underway to more quantitatively understand the results described above.

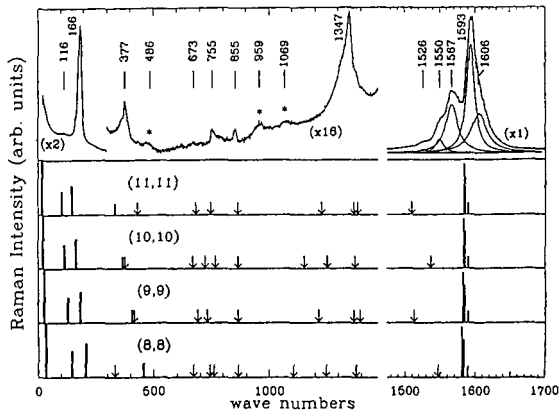


Fig. 3: Raman spectrum (top panel) of a SWNT sample taken using 514.5 nm excitation at  $\sim 2 \text{ W/cm}^2$ . The "\*" in the spectrum indicates features that are tentatively assigned to second-order Raman scattering. The four bottom panels are the calculated Raman spectra for armchair  $(n,n)$  nanotubes,  $n = 8 - 11$ . The downward-pointing arrows in the lower panels indicate the positions of the remaining weak, Raman-active modes [1].

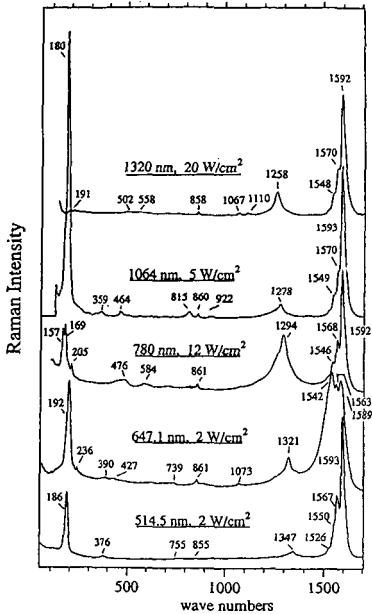


Fig. 4: Room-temperature Raman spectra for purified SWNTs, excited with five different laser frequencies. The power density for each spectrum is indicated, as are the vibrational frequencies.

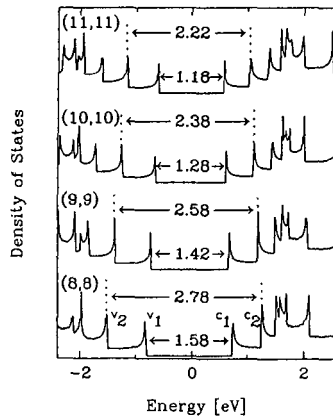


Fig. 5: Electronic density of states (DOS) calculated using a tight-binding model for  $(8,8)$ ,  $(9,9)$ ,  $(10,10)$ , and  $(11,11)$  nanotubes. The Fermi energy  $E_F$  is located at 0 eV. Wavevector-conserving optical transitions can occur between mirror-image spikes, e.g.,  $v_1 \rightarrow c_1$  and  $v_2 \rightarrow c_2$ .

## Acknowledgements

The author wishes to thank the NSF and DOE for his support during the course of this research. This paper is based on many of the results to appear in Ref. 1 and represents the fruits of a dynamic, multi-university collaboration between experimentalist and theoreticians.

## REFERENCES:

- [1] A. M. Rao, E. Richter, S. Bandow, B. Chase, P. C. Eklund, K. A. Williams, S. Fang, K. R. Subbaswamy, M. Menon, A. Thess, R. E. Smalley, G. Dresselhaus and M. S. Dresselhaus, *Science* (in press)
- [2] D. S. Bethune et al., *Nature* 363, 605 (1993).
- [3] S. Iijima and T. Ichihashi, *Nature* 363, 603 (1993).
- [4] For more details on carbon nanotubes see "*Science of Fullerenes and Carbon Nanotubes*" by M.S. Dresselhaus, G. Dresselhaus, and P. C. Eklund, Academic Press, New York, NY 1996.
- [5] A. Thess et al., *Science*, 273, 483 (1996).
- [6] R. A. Jishi et al., *Chem. Phys. Lett.*, 209, 77 (1993).
- [7] E. Richter and K. R. Subbaswamy (unpublished).
- [8] W. Hayes and R. A. Loudon, in *Light Scattering by Crystals*, (Wiley, New York, NY 1978).

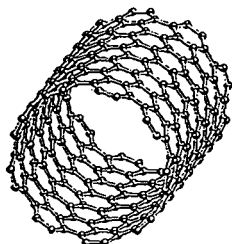


Fig. 1: Schematic model of a seamless (9,9) nanotube.

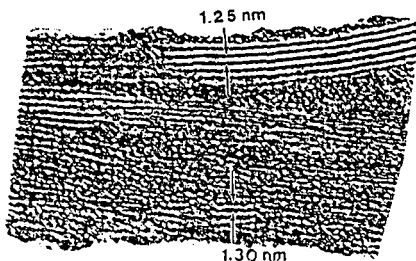


Fig. 2(a): Bright-field TEM image of a nanotube bundle. The bundles are found to be organized in triangular lattices. The arrows indicate measured approximate diameters of nanotubes within two bundles.

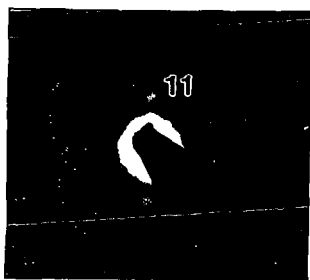


Fig. 2(b): Electron diffraction pattern with  $d_{11}$  spots corresponding to the diameter of an isolated nanotube.

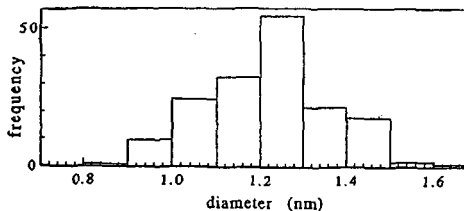


Fig. 2(c): Nanotube-diameter distribution tabulated from bright-field TEM images.

TABLES

TABLE I. First-order Raman-active vibrational mode frequencies in  $\text{cm}^{-1}$  for single-wall carbon nanotubes (SWNT): Experimental (514.5 nm excitation) and calculated. The experimental frequencies vary with laser excitation wavelength (see text and Fig. 4). The SWNT sample is thought to be an ensemble of  $n = 8 - 11$  armchair nanotubes.

Expt.		Ident. $n^b$	Sym. <sup>a</sup>	Theory <sup>c</sup>			
$\omega_0$	$I^d$			(8,8)	(9,9)	(10,10)	(11,11)
-			$E_{2g}$	34	27	22	18
116	w	10	$E_{1g}$	146	130	117	106
186	s	8,9,10	$A_{1g}$	206	183	165	150
377(s)	m	10 <sup>e</sup>	$E_{2g}$	333	-	368	-
377(b)	m	9,10 <sup>e</sup>	$E_{2g}$	458	408	371	335
-		-	$E_{1g}$		420		431
673	w	8,10	$A_{1g}$	671	-	670	-
-		-	$E_{1g}$	-	690	-	683
-		-	$E_{2g}$	-	732	-	746
-		-	$E_{2g}$	742	-	722	-
755	w	8,10	$E_{1g}$	762	-	766	-
855	w	8,9,10,11	$E_{2g}$	866	866	866	866
-		-	$E_{2g}$	1106	-	1152	-
-		-	$E_{1g}$	-	1216	-	1229
-		-	$A_{1g}$	1247	-	1252	-
1347	m	$\left\{ \begin{array}{l} 9, 11 \\ 8, 10 \end{array} \right.$	$A_{1g}$	-	1369	-	1369
			$E_{1g}$	1377	-	1374	-
1526	w	9,11	$E_{1g}$	-	1513	-	1510
1550	m	10	$E_{2g}$			1543	
1567	s	8	$E_{2g}$	1547	-	1531	-
1593	$\left. \begin{array}{l} s \\ m \end{array} \right\}$	$\left\{ \begin{array}{l} 8, 9, 10, 11 \\ 8, 9, 10, 11 \\ 8, 9, 10, 11 \end{array} \right.$	$A_{1g}$	1583	1584	1585	1586
1609			$E_{1g}$	1581	1582	1584	1585
			$E_{2g}$	1589	1589	1590	1590

<sup>a</sup>Mode symmetry as determined by model calculation.

<sup>b</sup>The  $n$  values of the armchairs nanotubes ( $n, n$ ).

<sup>c</sup>Empirical force constant model, see text.

<sup>d</sup>Intensity: w = weak, m = moderate, s = strong.

<sup>e</sup>This line at  $377 \text{ cm}^{-1}$  is a superposition of a broad (b) and a sharp (s) peak.

# Carbon Materials From Coal

Frank Derbyshire

Center for Applied Energy Research  
3572 Iron Works Pike  
University of Kentucky  
Lexington, KY 40511-8433

**Keywords:** coal, conversion, carbon materials

## INTRODUCTION

The production and consumption of coal is overwhelmingly directed to its use as a fuel for the generation of heat and power. At the same time, coal also represents a significant resource for the production of chemicals and carbon materials. Although, in this context, the current importance enjoyed by coal is much less than in former times, it can be anticipated that the non-fuel uses of coals will increase in years to come: coal is the most abundant fossil fuel; it is globally available; it is obtained at low cost; and the structure of coal is suited to the production of a broad range of products.

This paper will consider how the structure and composition of coals of different rank and origin can give rise to carbon materials with very different properties and fields of application. While the markets for these products can only have a small direct impact on coal consumption, they can exert a considerable indirect influence through materials applications that enhance the clean efficient use of energy. Examples include the control of emissions through adsorption and catalysis, energy storage devices and delivery systems, and the fabrication of strong lightweight structures for various forms of transport.

## STRUCTURE OF COAL AND CARBONS

The ability to produce a spectrum of carbons from coal can best be understood in relation to its basic structure. As depicted in a model developed by Oberlin<sup>1</sup>, coal consists of relatively low molecular weight structural units that are connected by different types of chemical bond. The structural units tend to be planar and consist of cyclic carbon (aromatic and hydroaromatic) and heterocyclic rings. Attached to the rings are alkyl, and oxygen and sulphur-containing groups. The structural units are connected by covalent (alkyl, or etheric - oxygen, and sulphur - bridges) and non-covalent bonds, hydrogen bonds and van der Waals forces. A proportion of weakly bonded or physically trapped material is also present, some of which can be extracted by solvents. While the overall structure is amorphous, there are limited regions of short-range order that are defined by the parallel alignment of two (or more) structural units.

As the rank of the coal increases, there are changes to the structure that include: an increase in aromaticity and a reduction in aliphatic content; the elimination of oxygen functionalities; and changes in the nature of the connecting linkages between structural units - a decrease in the extent of hydrogen bonding and covalent linkages, and an increase in aromatic-aromatic interactions<sup>2,3</sup>. There are accompanying changes in the spatial arrangement of the structural units that improve the extent of short-range order: increases in the average number of atoms per structural unit, in the number of structural units or layers that are aligned in parallel, and in the mutual orientation of sets of parallel layers<sup>4</sup>. The model predicts, as confirmed by other studies, that coals possess inherent porosity, and that with increasing rank, the pore structure becomes narrower.

For the production of some carbon materials, coal serves simply as a source of elemental carbon and its structure and composition are not of any great relevance. These processes tend to involve high energy input, and the rearrangement of carbon atoms and carbon fragments in the vapor phase, or via vapor-solid reaction, to produce highly ordered carbons such as fullerenes and nanotubes<sup>5,6</sup> and filaments<sup>7</sup>. However, in the majority of cases, the conversion process takes advantage of the structure of coal with the aim either of preserving its amorphous configuration or of promoting increased structural order.

With the exceptions of diamond, diamond-like materials, and closed-cage structures (fullerenes and nanotubes), the structure of most carbons is related to that of crystalline graphite. Nascent elements of the graphite structure are recognizable in coal in the form of planar cyclic carbon structures, and their propensity for parallel orientation. Upon the thermal treatment of coals (or any other solid or liquid carbonaceous precursor) the thermodynamic driving force is towards improved structural order through the aromatization, growth and alignment of structural units. The potential for ultimately producing a graphitic structure is determined by the changes that occur between about 400-600°C, as illustrated in Figure 1. The formation of crosslinks between structural units can impede improvements in structural order, preserving the random order present in the parent coal, and resulting in a hard, porous, isotropic char. Such materials are termed non-graphitizing carbons, as there is little further improvement in crystalline growth and ordering upon heat treatment to temperatures as high as 3000°C. Low-rank coals, oxidized bituminous coals, and anthracites follow this pathway.

Under conditions where there is minimal crosslinking, the formation of a fluid state allows planar aromatic structures to grow in size and diffuse into positions of parallel alignment, leading to the nucleation and growth of a separate anisotropic phase within the parent isotropic liquid. The anisotropic phase is a liquid crystal known as carbonaceous mesophase. If continued, the process is eventually arrested by solidification of the melt. The anisotropic carbon content of the resulting char is determined by the precursor composition and carbonization conditions, and the duration of the fluid phase. In the carbonization of (bituminous) coking coals and coking coal blends, mesophase development is limited because, in the coke oven, there is a mixture of fluid and solid phases, and the heating conditions are such that the existence of the plastic condition is transient. The char or coke consists of a mixture of isotropic, and small and larger anisotropic regions: in the terminology of optical microscopy, mosaic and flow domains, respectively. With pitch precursors, a fluid condition can be maintained for longer periods, allowing the possibility of extensive mesophase development through the continued formation of nuclei, their growth and coalescence. The highly anisotropic chars thus produced are composed of small, well-ordered pseudo-graphitic crystallites that are oriented with their basal planes in approximately parallel orientation. They are weaker, due to the low density of crosslinks, and are of lower porosity than isotropic chars produced from thermosetting precursors. These are graphitizing carbons, which experience a sharp improvement in structural order and crystallite size upon heat treatment to temperatures above about 2200°C.

## DIRECT CONVERSION OF COALS TO CARBONS

### Activated Carbon

In the production of activated carbons from coal, it is desirable to preserve, as far as possible, the amorphous nature of the parent coal structure: the porosity of activated carbons derives from the small size of the constituent disordered crystallites and their random packing. As discussed, this is achieved via crosslinking reactions during low-temperature carbonization. Low-rank coals and anthracites can be processed directly, while the thermoplastic behavior of bituminous coals is first suppressed by air oxidation, or other means such as the use of additives or coal blending.

Coals are carbonized at 500 - 700°C to produce isotropic chars with pore structures that reflect those of the starting coals. However, partly because of volume contraction that is caused by heat treatment, most of the pores are closed or too narrow to be of practical value. Porosity is then developed by activation in which carbon is removed through controlled gasification at 800-1000°C in steam or CO<sub>2</sub>. The pore structure in the final carbon product is therefore not created but is a development of the basic structure that is inherent to the starting material and translates through the processes of carbonization and activation. For this reason, activated carbons produced from coals of different rank reflect the same changes in pore size distribution as do the original coals: those from low-rank coals have high mesopore volumes, those from bituminous coals have a broad pore size distribution, and those from high rank coals are microporous. Together, coals and lignite constitute about 50% of the raw materials used to manufacture activated carbons. They are produced with a broad range of product properties, in the form of both powders and larger sized products (granules, pellets or extrudates).

Activated carbons with novel properties can be produced from coal by chemical activation using KOH. Extremely high surface area carbons can be produced from bituminous coals and petroleum coke precursors by reaction with KOH at temperatures up to 1000°C, followed by leaching to recover the reagent<sup>8</sup>. Despite the unusual properties of this activated carbon (surface area > 3000 m<sup>2</sup>g<sup>-1</sup>, and total pore volume 2.0 - 2.6 ml/g), only limited quantities have been produced. The cost, low bulk density, and difficulties in handling have presented obstacles to successful commercialization, although a recent development has allowed the powder to be incorporated into a more tractable monolithic form<sup>9</sup>. In variants of the same process, KOH has also been used to produce high surface area, hard extruded carbons from low-rank coals<sup>10</sup> and preoxidized bituminous coals<sup>11</sup>, high surface area activated mesocarbon microbeads (see below)<sup>12,13</sup>, and catalysts with high activity and selectivity for the hydrodehalogenation of halogenated aromatic compounds - reactions that are of interest for environmental protection<sup>14,15</sup>.

### Metallurgical Coke

The manufacture of metallurgical coke represents the single largest non-fuel use of coal for the production of a carbon material, accounting for approximately 10% of world coal consumption. The phenomenon of fluidity development in coking coals and coking coal blends is critical to producing the characteristics required of metallurgical coke. An associated outcome is the development of anisotropy through mesophase formation. Its significance to many of the properties of coke that are of importance to metallurgical practice is a matter of some debate, but it does appear to influence coke strength<sup>16</sup>.

## CARBONS FROM COAL-DERIVED LIQUIDS

The range of carbons that can be obtained from coal is considerably expanded through the derivation of high molecular weight liquids or pitches. Liquids can be obtained by a number of different methods, such as solvent extraction, hydrolysis, direct liquefaction, and coking, each of which effectively serves to liberate the coal structural units. The composition of the liquids can be altered to a greater extent through the selection of the coal and reaction parameters, allowing

considerable latitude in the preparation of precursors for different end-products.

### **Isotropic and Mesophase Pitch Carbon Fibers**

Different types of carbon fibers can be classified according to the precursor or process method: polymers, rayon and polyacrylonitrile (PAN); vapor-grown; and pitch. The last of these groups is divided into fibers produced from isotropic pitch, and from pitch that has been pretreated to introduce a high concentration of carbonaceous mesophase. The former are so-called general purpose fibers that are sufficiently strong to be used in a wide range of applications, while the latter are high performance materials, possessing very high tensile strength and modulus. Extensive discussions of the synthesis and applications of isotropic pitch-based and mesophase pitch-based carbon fibers has been given by Edie<sup>17</sup>, and Singer<sup>18</sup> has written a more general account of carbon fiber technology.

The production of isotropic pitch-based carbon fibers by melt-blowing was first commercialized in 1970, using a pitch prepared from ethylene cracker tar. Subsequently, commercial processes were developed to produce isotropic fibers from coal-tar pitch, and petroleum pitch prepared from decant oils produced by fluidized catalytic cracking<sup>see 19</sup>. During the 1970's, the National Coal Board (now the British Coal Corporation), United Kingdom, conducted extensive research on the formation of continuous carbon fibers from coal extracts produced by a liquid solvent extraction process, LSE<sup>20</sup>. Although the starting material was isotropic, the aim was to produce fibers with high strength and modulus, and a final high temperature heat treatment step under tension was used to improve fiber strength - a technique that has also been applied to rayon-based and isotropic pitch carbon fibers<sup>18</sup>. Although these fibers were unable to compete with the later-developed PAN and mesophase fibers, the work demonstrated that other sources of coal liquids could be used as effective fiber precursors. Recent work has shown that continuous filaments of isotropic carbon fibers can be produced from coal liquefaction products<sup>21,22</sup>.

The discovery of carbonaceous mesophase in the 1960s<sup>17,18</sup> led to the development of mesophase fibers, in which the orientation of the molecular structure along the fiber axis allows the development of a graphitic structure. Because the intermolecular interactions in the liquid crystal phase are so weak, they can be oriented by any small shear force such as in extrusion or elongation, to produce an oriented fiber. Moreover, the orientation and resulting structure can be modified by spinning conditions, and especially the spinnerette design.

The preparation of the starting material for isotropic and mesophase pitch fibers involves quite different treatments. For isotropic pitch fibers, the principal steps involve the removal of volatile components by distillation, and solids separation. Distillation increases the softening point and aromaticity of the pitch. For mesophase fibers, the pitch must be further treated in one of several different ways to generate a high mesophase content product that is suitable for melt spinning. Spinnability is a critical requirement, since the production of continuous filaments is essential for most applications of high performance fibers. In both cases, the as-formed, "green" fibers require to be stabilized to render them thermosetting before carbonization. Stabilization is normally accomplished by air oxidation, with a weight gain of up to 10%. The introduction of oxygen functionalities leads to the formation of crosslinks during oxidation and subsequent carbonization. Oxidation must be initiated at temperatures below the glass transition temperature of the fibers to prevent melting, and for mesophase fibers, to prevent loss of molecular orientation. With continuing reaction, oxidative crosslinking progressively raises the glass transition temperature, such that the reaction temperature (and rate) can be increased. Eventually, the glass transition temperature is sufficiently elevated that pyrolysis reactions precede plasticity development, and the fibers can be carbonized.

To develop strength, the stabilized fibers are carbonized in inert atmosphere at temperatures up to about 1200°C. This is the final chemical processing step for isotropic fibers: due to the lack of molecular orientation, there is little further gain in strength upon heat treatment to higher temperatures. Conversely, there are large increases in the tensile strength and modulus of mesophase fibers upon graphitization (up to 3000°C). The final fiber properties are determined by the degree of orientation of layer planes along the fiber axis, and the size and perfection of individual crystallites. The modulus of isotropic fibers is about 1/20 of that of mesophase fibers, while their tensile strength is around 1/3.

Lower cost makes isotropic pitch fibers attractive for applications where high tensile strength or modulus are not required. Examples include: enhancing the properties of composite friction materials; the reinforcement of engineering plastics; ablation materials; acoustic and thermal insulation; electrically conductive fillers for polymers; electromagnetic shielding; filter media; paper and panels; the production of hybrid yarns with other fibers; reinforcing concrete to improve flexural strength and other properties; and as potential replacements for asbestos. Mesophase pitch fibers are used in advanced composite materials. Graphitized mesophase pitch fibers tend to have higher modulus and lower tensile strength than the PAN-based equivalents: the former have advantages in applications requiring high stiffness, high electrical and thermal conductivity, low thermal expansion, and high temperature oxidation resistance, while the latter are employed where high strength is required. Because of their high modulus, mesophase fibers are often used in

aerospace structures, and the very high thermal conductivity of recently developed fibers has opened applications for heat dissipation in areas such as high speed machinery, aircraft structures, and electronics.

### Activated Carbon Fibers

There is a growing interest in the development and application of activated isotropic carbon fibers (ACF). They can be produced with high surface area, and the narrow fiber diameters (usually 10 to 20 microns) lead to much faster adsorption, desorption, or catalytic reaction than for granular carbons. The novel properties of ACFs make them more attractive than other, more conventional activated carbons for certain applications<sup>19</sup>. In this laboratory, we have examined the synthesis of isotropic pitch fibers and activated fibers from non-conventional pitches. Whereas most commercial ACFs are microporous, activated carbon fibers produced from shale oil asphaltenes and from coal liquefaction products are found to possess high mesopore volumes<sup>21,22</sup>. Through the selection of appropriate precursor pitches, it is possible to produce ACFs with substantially different properties in terms of pore size distribution and surface chemistry, as well as potentially allowing more rapid processing. In this context, coals present a fertile resource as heavy coal liquids can be produced relatively cheaply, and with a wide range of composition.

Individual fibers (and powders) present difficulties in handling, containment, and regeneration, and in fixed bed operations they would present an unacceptably high pressure drop. These problems can be surmounted by their incorporation into forms such as felt, paper, woven and nonwoven fabrics, and rigid monolithic structures. Potential advantages of the monolithic forms are: they allow facile handling; they can be highly permeable; they permit the possibility of regeneration; where there is good contact between the carbon constituents and if they are adequately conducting, electrical energy can be used as a method of rapid and uniform heating to drive the processes of desorption or regeneration<sup>23-26</sup>; and they can be fabricated to a given size and shape, a consequence of which is that completely novel adsorber/ reactor designs are possible.

In this laboratory, we have developed rigid activated carbon fiber composite materials<sup>27,28</sup>. Using pre-activated carbon fibers, 80-90% of the surface area of the free fibers is retained in the composite. Alternately, the formed composite can be carbonized and activated in steam or carbon dioxide. The composites are strong, highly permeable to fluids, and can be machined. They can be used to efficiently separate CH<sub>4</sub> and CO<sub>2</sub><sup>28</sup>. In liquid and gas phase column tests, the composites have been compared to commercial granular activated carbons, where it has been found that there is much more effective use of the adsorptive capacity of the carbon before column breakthrough. The higher efficiency of the composite is attributed to: the uniform structure which ensures that the feed is distributed evenly through the column: the presentation of the adsorbent surface in fiber form which allows high rates of adsorption; and the open architecture which renders the pore structure readily accessible.

### Mesocarbon Microbeads

By arresting the process of mesophase development at the nucleation stage, mesophase microbeads can be obtained by separation using techniques such as centrifugation and solvent extraction. The diameter of the beads is typically in the range 1 - 80  $\mu\text{m}$ <sup>12,13</sup>. The microbeads are used in the "green" form to produce so-called sintered or binderless carbons<sup>29</sup>. These are high density, high strength, shaped carbons that are formed by molding the microbeads. Upon carbonization, strong bridging bonds are created at the points of contact between the microbeads. Under applied pressure, deformation of the microbeads helps to minimize the porosity of the resulting artefact. Heat treatment to graphitizing temperatures greatly enhances strength and produces a material that is composed of graphitic microbeads but is macroscopically isotropic due to their random orientation. Carbonized and graphitized microbeads are used in the production of new composite materials, including electrode materials for Lithium batteries. The various applications of the microbeads take advantage of the basic properties of graphite - high resistance to corrosion and oxidation, and excellent electrical and thermal conductivity.

### Needle Coke

Highly anisotropic cokes are obtained by solidification after extensive mesophase development. The structure renders them relatively friable or "soft", with low porosity, and the anisotropy is reflected in the acicular shape of the coke particles, which are termed needle coke. Needle cokes are readily graphitizable and are used for the manufacture of graphite electrodes for arc-steel furnaces. Normally, needle coke is produced from selected petroleum feedstocks: one example is decant oils from fluid catalytic cracking. Feedstock properties such as high aromatic carbon content are important. The aromatic character of coals implies that they could present an attractive alternative source for the production of needle coke, and it has been shown that highly aromatic, pretreated coal tar pitches can give excellent needle cokes. It has further been demonstrated that a suitable needle coke can be obtained from coal via solvent extraction<sup>30</sup>. Bituminous coal is slurried with about three times its mass of anthracene oil (itself a product of coal tar distillation), and heated to 415°C for 60 min at 0.8 MPa (autogenous pressure), when approximately 70-80% of the coal (dmmf) is solubilized. The mineral matter and undissolved coal are separated by hot pressure filtration to afford a coal extract solution (filtrate) containing around 0.1% ash. The extract is then preheated to ~ 520°C and fed to a delayed coker to produce needle coke, and the coker overhead is

recycled as solvent. The process has been successfully demonstrated on a large scale in which sufficient coke was produced to fabricate graphite electrodes (using coal tar pitch binder) that were tested in a 25 ton steel production furnace<sup>30</sup>. Approximately 10% of needle coke is now produced from pretreated coal tar: annual world production is about 1.3 Mt.

**REFERENCES**

1. Oberlin A (1989) In: Chemistry and Physics of Carbon, 22 (Ed. P. A. Throver), Marcel Dekker 1989, 1-143.
2. Nishioka M, Larsen J W (1990) Energy & Fuels, 4 (1), 100-106.
3. Barton W A, Lynch L J (1989) Proc. Int. Conf. Coal. Sci. Tokyo, 13-16.
4. Cartz L, Hirsch P B (1960) Phil. Trans. R. Soc., 252, 557-602.
5. Howard J B et al (1991) Nature, 352, 139-141.
6. Wilson M A, Pang L S K, Quezada R A (1995) Proc. Eighth International Conference on Coal Science (Eds. J. A. S. Pajares and J. M. D. Tascón), 2, Elsevier, 1177-1180.
7. Burton D, Lake M, Alig R (1996) Am.Chem.Soc.Div.Fuel Chem. Preprints, 41(1), 349-353.
8. Wennerberg A N, O'Grady T M (1978) US Patent 4,082,694.
9. Robinson, K, Mieville, R (1996) Megacarbon Inc., personal communication
10. Guy P J et al (1989) Proc. Int. Conf. Coal. Sci. Tokyo, 23-27.
11. Verheyen V et al (1995) Carbon, 33 (6), 763-772.
12. Kasuh, T, Morino, G (1992) US Patent 5,143,889
13. Matsumura, Y, Maeda, T (1992) Tanso, 155, 403-406.
14. Farcasiu M et al (1994) J. Catal., 146, 313-316.
15. Kaufman P B et al (1996) Am.Chem. Soc. Div. Fuel Chem. Preprints, 41 (1), 447-450.
16. Patrick, J W, Reynolds, M J, Shaw, F H (1982) Proc. 64th CIC Coal Symposium (A. M. Al Talweel, Ed.), C. S. Ch. E., 550-559.
17. Edie, D D (1990) In: Carbon Filaments and Composites (J. L. Figueredo et al, Eds.), Kluwer Academic Publishers, 43-72.
18. Singer, L S (1994) In: Materially Speaking, 9 (2), Materials Technology Center, Southern Illinois University at Carbondale, IL, USA.
19. Derbyshire, F J et al (1994) Am.Chem. Soc. Div. Fuel Chem. Preprints, 39 (1), 113-120.
20. Jorro, M A A, Ladner, W R (1974) Proc., 4th Int. Carbon Conference, London, Sept., 287.
21. Fei Y Q et al (1993) Proc. Eastern Oil Shale Symposium, Lexington, KY, Nov. 16-19, 38-45.
22. Kimber et al (1996) Proc. Pittsburgh Coal Conference, 553-558.
23. Economy J et al (1996) Am.Chem. Soc. Div. Fuel Chem. Preprints, 41 (1), 321-325.
24. Lordgooei M et al (1996) Am.Chem. Soc. Div. Fuel Chem. Preprints, 41 (1), 369-373.
25. Kimber G M, Johnson A (1996) Proc. European Carbon Conference - Carbon '96, Newcastle, UK, July, 52-53.
26. Le Cloirec P et al (1996) Am.Chem. Soc. Div. Fuel Chem. Preprints, 41 (1), 379-384.
27. Jagtoyen M et al (1994) Materials Research Society Symposium Proceedings, 344, 77-81.
28. Kimber G M et al (1996) Gas Sep. Purif., 10 (2), 131-136.
29. Dollin, P, Ting, D N, Rand, B (1996) Proc. European Carbon Conference - Carbon '96, Newcastle, UK, July, 421-422.
30. Kimber, G M, Brown, A, Kirk, J N (1981), High Temperatures-High Pressures, 13, 133-137.

**Figure 1. Production of disordered and ordered carbons from coal**

